UNIVERSIDADE D
COIMBRA

José Pedro Alvarinhas Batista

Maximising Non-Linear Optical Response Of Molecules

Insights From Model 1D-Systems

VOLUME 1

Dissertação no âmbito do Mestrado em Física, ramo de Física da Matéria Condensada orientada pelo Professor Doutor Fernando Manuel Silva Nogueira e apresentada ao Departamento de Física da Faculdade de Ciências e Tecnologia

Setembro de 2021

Maximising Non-Linear Optical Response Of Molecules

Insights From Model 1D-Systems

José Pedro Alvarinhas Batista

A thesis submitted for the degree of
Master in Physics

Department of Physics
University of Coimbra
Portugal
September 2021

Abstract

The first hyperpolarizability tensor β is a central quantity for several technological applications, and its maximization in one-dimensional systems has been a target for numerical optimizations in an attempt to gain insight into how to build linear-chain molecules with the largest response possible. Previous work by Kuzyk et. al. has shown that a limit for the intrinsic hyperpolarizability (β_{int}), the quotient between the hyperpolarizability of the system (β) and the maximum hyperpolarizability within a 3-level ansatz assumed to optimize the non-linear response (β_{max}), appears to exist, and that within that framework and the models for interaction considered the universal properties observed in the non-interacting systems are preserved in the interacting ones. In this work we do an optimization procedure for these one-dimensional systems using a genetic algorithm and working within the framework of TDDFT (Time-Dependent Density Functional Theory) in order to study what happens when going from a two non-interacting electron system to an interacting one. The goal for this study is to see how the presence of interaction changes not only the values of β but also the behavior of the system's wavefunctions and potential. With this approach we are able to find that when interactions are turned on there is a sharp (11 orders of magnitude) increase on the maximum value of $|\beta|$, the wavefunction becomes more localized in one of the regions of the potential and that region itself becomes wider when compared to the non-interacting case.

Resumo

O tensor da primeira hiperpolarizabilidade β é uma quantidade central para diversas aplicações tecnológicas, tendo a sua maximização em sistemas unidimensionais vindo a ser um alvo para otimizações numéricas numa tentativa de compreender como construir moléculas lineares com a maior resposta possível. Trabalhos anteriores de Kuzyk et. al. provaram a existência de um limite para a hiperpolarizabilidade intrínseca (β_{int}), o quociente entre a hiperpolarizabilidade do sistema (β) e a hiperpolarizabilidade máxima dentro da ansatz de 3-níveis que se assume que otimiza a resposta não linear (β_{max}), aparenta existir, e que dentro desse framework e com os modelos considerados para modelar a interação, as propriedades universais observadas nos sistemas não-interatuantes são preservadas nos interatuantes. Neste trabalho é feito um processo de otimização para estes sistemas unidimensionais usando um algoritmo genético e trabalhando dentro do framework da TDDFT (Time-Dependent Density Functional Theory) por forma a estudar o que acontece quando se passa de um sistema de dois eletrões não-interatuantes para um interatuante. O objetivo para este estudo é verificar como é que a presença de interação muda não só os valores de β como também o comportamento das funções de onda e do potencial do sistema. Com esta abordagem conseguimos verificar que quando as interações são ligadas há um aumento brusco (11 ordens de grandeza) no valor máximo de $|\beta|$, a função de onda torna-se mais localizada numa das regiões do potencial e essa mesma região é alargada em comparação com o caso não-interatuante.

Contents

Contents **ix**

1 An Overview On TDDFT **1**
1.1 Runge-Gross Theorem 1
1.2 Time-Dependent Kohn-Sham Equations 8
1.3 Linear Response In TDDFT 9
1.4 Higher-Order Response 13
1.5 The Sternheimer Method 14

2 Genetic Algorithms **19**

3 State Of The Art **21**

4 Results And Discussion **25**
4.1 The Genetic Algorithm 25
4.2 TDDFT Calculations 27
4.3 Results 27

5 Conclusions And Future Work **34**

Appendices **35**

A Density Functional Theory **36**
A.1 The Hohenberg-Kohn Theorem 36
A.2 The Kohn-Sham Scheme 39
A.3 The Local Density Approximation 40

B Hall Of Fame From The Genetic Algorithm's Optimization **42**

References **53**

Chapter 1

An Overview On TDDFT

1.1 Runge-Gross Theorem

The time evolution of a system of N interacting non-relativistic electrons is determined by the time-dependent Schrödinger equation:

$$\hat{H}(t)\Psi(\boldsymbol{x}_1, \boldsymbol{x}_2, ..., \boldsymbol{x}_N, t) = i\frac{\partial}{\partial t}\Psi(\boldsymbol{x}_1, \boldsymbol{x}_2, ..., \boldsymbol{x}_N, t) = E\Psi(\boldsymbol{x}_1, \boldsymbol{x}_2, ..., \boldsymbol{x}_N, t) \tag{1.1}$$

with (in the Born-Oppenheimer approximation)

$$\hat{H}(t) = \hat{T} + \hat{V}_{ee} + \hat{V}_{ext}(t), \tag{1.2}$$

$\Psi(\boldsymbol{x}_1, \boldsymbol{x}_2, ..., \boldsymbol{x}_N, t)$ the N-fermion wavefunction and E the eigenvalues of the Hamiltonian operator $\hat{H}$. We use the shorthand notation $\boldsymbol{x}_i \equiv (\boldsymbol{r}_i, \sigma_i)$ for the space and spin coordinates of the ith electron, and units of $c = \hbar = 1$. In both the time-dependent and time-independent cases, the kinetic energy and electron-electron interaction energy operators $\hat{T}$ and $\hat{V}_{ee}$ are given by (choosing the Coulomb interaction for $\hat{V}_{ee}$):

$$\hat{T} = -\frac{1}{2}\sum_{i=1}^{N}\nabla_i^2 \tag{1.3}$$

$$\hat{V}_{ee} = \frac{1}{2}\sum_{i\neq j}^{N}\frac{1}{|\boldsymbol{r}_i - \boldsymbol{r}_j|}. \tag{1.4}$$

On the other hand, the external potential $\hat{V}_{ext}$ differs between both cases: in the time-independent case we write

$$\hat{V}_{ext} = \sum_{i=1}^{N} v_{ext}(\boldsymbol{r}_i), \tag{1.5}$$

while in the time-dependent case

$$\hat{V}_{ext} = \sum_{i=1}^{N} v_{ext}(\boldsymbol{r}_i, t). \tag{1.6}$$

Solving equation (1.1) and thus obtaining the exact N-electron wavefunction would lead to the knowledge of the expectation value of every time-dependent observable of the system. This comes from the fact that for a given time-dependent operator $\hat{\mathcal{O}}(t)$, the corresponding observable $\mathcal{O}(t)$ is given by

$$\mathcal{O}(t) = \langle \Psi(t) | \hat{\mathcal{O}}(t) | \Psi(t) \rangle, \tag{1.7}$$

where the space-spin dependency is omitted in Ψ. The N interacting electron problem can therefore be seen as the problem of finding the N-electron wavefunction, as this is the object which will allow us to bridge the gap between the operators, which are general, and the system.

In the case of the time-independent Schrödinger equation, the simplest approach to the problem is to assume that Ψ is a Slater determinant of the one-electron orbitals, i.e. the simplest fermionic wavefunction one can write:

$$\Psi(\boldsymbol{x}_1, \boldsymbol{x}_2, ..., \boldsymbol{x}_N) = \frac{1}{\sqrt{N!}} \begin{vmatrix} \varphi_i(\boldsymbol{x}_1) & \varphi_j(\boldsymbol{x}_1) & ... & \varphi_k(\boldsymbol{x}_2) \\ \varphi_i(\boldsymbol{x}_2) & \varphi_j(\boldsymbol{x}_2) & ... & \varphi_k(\boldsymbol{x}_2) \\ ... & ... & & ... \\ \varphi_i(\boldsymbol{x}_N) & \varphi_j(\boldsymbol{x}_N) & ... & \varphi_k(\boldsymbol{x}_N) \end{vmatrix}. \tag{1.8}$$

Here $\frac{1}{\sqrt{N!}}$ is a normalization factor so that the integral over all space of $|\Psi|^2$ is 1, and φ are one-electron orbitals, each of them being a solution of the one-electron Schrödinger equation. This Ψ leads us to a simplified form of the expectation value of $\hat{H}$,

$$\begin{aligned} \langle \Psi | \hat{H} | \Psi \rangle &= \sum_{i=1}^{N} \langle \varphi_i | \hat{T} + \hat{V}_{ext} | \varphi_i \rangle + \sum_{i \neq j}^{N} \langle \varphi_i | \hat{V}_{ee} | \varphi_i \rangle \\ &= \sum_{i=1}^{N} \int \varphi_i(\boldsymbol{x}) \left(-\frac{\nabla^2}{2} + v_{ext}(\boldsymbol{r}_i) \right) \varphi_i(\boldsymbol{x}) d\boldsymbol{x} + \frac{1}{2} \sum_{i,j=1}^{N} (J_{ij} - K_{ij}), \end{aligned} \tag{1.9}$$

with $J = 1/2 \sum_{i,j=1} J_{ij}$ the classical electrostatic repulsion energy and $\sum_{i,j=1} K_{ij}$ the exchange energy, given by

$$J_{ij} = \int \varphi_i(\boldsymbol{x}_1) \varphi_i^*(\boldsymbol{x}_1) \frac{1}{|\boldsymbol{r}_i - \boldsymbol{r}_j|} \varphi_j(\boldsymbol{x}_2) \varphi_j^*(\boldsymbol{x}_2) d\boldsymbol{x}_1 d\boldsymbol{x}_2 \tag{1.10}$$

$$K_{ij} = \int \varphi_i^*(\boldsymbol{x}_1) \varphi_j(\boldsymbol{x}_1) \frac{1}{|\boldsymbol{r}_i - \boldsymbol{r}_j|} \varphi_i(\boldsymbol{x}_2) \varphi_j^*(\boldsymbol{x}_2) d\boldsymbol{x}_1 d\boldsymbol{x}_2, \tag{1.11}$$

with

$$\int d\boldsymbol{x}_i = \sum_{\sigma_i} \int d\boldsymbol{r}_i \tag{1.12}$$

The Slater determinant Ψ that minimizes the expectation value $\langle\Psi|\hat{H}|\Psi\rangle$ is the Hartree-Fock wavefunction (Ψ_{HF}) and it describes the ground-state of the system within this approximation, with the self-consistent method used to calculate Ψ_{HF} known as the Hartree-Fock (HF) approximation. With φ_i being the HF single-particle wavefunctions, $|\Psi_{HF}\rangle$ is the lowest energy eigenfunction of the HF Hamiltonian:

$$\hat{H}_{HF} = \sum_i^N \left(-\frac{\nabla_i^2}{2} + v_{ext}(\boldsymbol{r}_i) + \frac{1}{2}\sum_j \int d\boldsymbol{x}_2 |\varphi_j(\boldsymbol{x}_2)|^2 \frac{1}{|\boldsymbol{r}_i - \boldsymbol{r}_j|} + \sum_j \hat{K}_j \right), \tag{1.13}$$

where the third term is the classical electrostatic energy operator (also known as the Hartree potential operator) and $\hat{K}_i$ is the exchange-energy operator defined by its action on φ_i:

$$\hat{K}_j \varphi_i(\boldsymbol{x}_1) = \int d\boldsymbol{x}_2 \varphi_j^*(\boldsymbol{x}_2) \frac{1}{|\boldsymbol{r}_i - \boldsymbol{r}_j|} \varphi_i(\boldsymbol{x}_2)\varphi_j(\boldsymbol{x}_1). \tag{1.14}$$

The problem with this approach is that to take $\Psi(t)$ as a simple Slater determinant is equivalent to neglecting most of the electron correlation (the remaining correlation is occurs when dealing with same-spin electrons), which is in no way a general statement one can make about a many-body system. Taking correlation into account, the exact $\Psi(t)$ can be written as a linear combination of all possible N-electron Slater determinants formed from a complete set of spin orbitals [16].

Although complex post-HFA methods like CI (Configuration Interaction) or MPPT (Møller-Plesset Perturbation Theory) exist, the issue of working with the wavefunction as an object does not stop at the fact that it has to be approximated for the N-electron case; in fact, one of the most crucial issues of these methods is that of the size of Ψ, as this object scales exponentially with the number of electrons, making systems beyond a given size not viable to analyze even computationally.

A major paradigm shift regarding this problem was done through the formulation of Density Functional Theory (DFT), that with its fundamental pieces (the Hohenberg-Kohn theorem and the Kohn-Sham scheme) manages to (for the ground-state of the system) not only change the problem into an artificial but equivalent one that is solved exactly by a Slater determinant, but also prove that any observable $\mathcal{O}$ can be written as an explicit functional of an object far simpler than Ψ: the electron-density.

Just as in ground-state DFT, the time-dependent version of DFT (TDDFT) arises as an alternative to solving the Schrödinger equation for the full many-body wavefunction, and its intention is again to reduce the exponential scaling with number of electrons that is associated with both equation (1.1) and its time independent version in order to make it viable computationally. This scaling is replaced by a N^3 one in DFT and TDDFT,

which allows for the study of much larger systems than would otherwise be possible with the same computational power.

Despite the fact DFT and TDDFT look very similar due to both being solved in the Kohn-Sham scheme, to derive TDDFT one must rely on entirely different theorems than the ones used in the ground-state case; it is neither the case that the time-dependent theorems are just generalizations of the ground-state ones nor that they necessarily reduce to them in a static case. The time-dependent case does however make very good use of ground-state DFT, as we will see many times below.

We start our showing of the foundations of TDDFT with the Runge-Gross theorem, which fulfills the role of the Hohenberg-Kohn theorem in the time-dependent case. Its statement is that for a given initial many-body state Ψ_0 there is a one-to-one mapping between the time-dependent external potential and the time-dependent one-particle electronic density, built from the many-body wavefunction $\Psi(t)$ from equation (1.1) as

$$n(\boldsymbol{r},t) = N\sum_{\sigma}\int d\boldsymbol{x}_2 ... \int d\boldsymbol{x}_N |\Psi(\boldsymbol{r},\sigma,\boldsymbol{x}_2,...\boldsymbol{x}_N,t)|^2, \tag{1.15}$$

with N the number of particles, so that the density is normalized to N. Just like in DFT (the only difference being the time-dependency), $n(\boldsymbol{r},t)$ represents the probability of finding an electron at position $\boldsymbol{r}$ and instant t, regardless of its spin. The proof here is done for the spin unpolarized case, with the spin polarized one being very similar.

To prove the aforementioned one-to-one mapping, the Runge-Gross theorem attempts to show that two time-dependent external potentials $v_{ext}(\boldsymbol{r},t)$ and $v'_{ext}(\boldsymbol{r},t)$, differing by more than a time-dependent function (which is the analogue of having two potential that differ by more than a constant in the ground-state theory) such that

$$v'_{ext}(\boldsymbol{r},t) \neq v_{ext}(\boldsymbol{r},t) + c(t), \tag{1.16}$$

acting on a system with a given initial state Ψ_0 will always lead to two different densities $n(\boldsymbol{r},t)$ and $n'(\boldsymbol{r},t)$. It is crucial to note that the initial state is not necessarily the ground-state nor any eigenstate of the initial potential, which means the case of a potential that is abruptly switched on is covered by the theorem.

This proof requires us to impose a crucial condition on the potentials: they are required to be time analytic, i.e., that we can expand them in a Taylor series centered around an initial time (that for the sake of simplicity we take to be $t_0 = 0$) such that

$$v_{ext}(\boldsymbol{r},t) = \sum_{k=0}^{\infty}\frac{1}{k!}v_{ext,k}(\boldsymbol{r})t^k. \tag{1.17}$$

Given the analytic form of the potentials, equation (1.16) is equivalent to saying that there exists an integer q beyond which (i.e., for $k \geqslant q$) $v'_{ext,k}(\boldsymbol{r})$ and $v_{ext,k}(\boldsymbol{r})$ differ by more than a constant. We are now in condition to proceed with the proof.

The first step is to prove that different external potentials lead to different current-densities $\boldsymbol{j}(\boldsymbol{r},t)$, with

$$\boldsymbol{j}(\boldsymbol{r},t) = \langle\Psi(t)|\hat{\boldsymbol{j}}(\boldsymbol{r})|\Psi(t)\rangle \tag{1.18}$$

and the paramagnetic current-density operator $\hat{\boldsymbol{j}}$

$$\hat{\boldsymbol{j}}(\boldsymbol{r}) = \frac{1}{2i}\sum_{i=1}^{N}[\nabla_i\delta(\boldsymbol{r}-\boldsymbol{r}_i) + \delta(\boldsymbol{r}-\boldsymbol{r}_i)\nabla_i]. \tag{1.19}$$

Applying the equations of motion of the expectation value of an operator in the Heisenberg picture to $\hat{\boldsymbol{j}}(\boldsymbol{r})$ and $\hat{\boldsymbol{j}'}(\boldsymbol{r})$, we get (since $\partial\hat{\boldsymbol{j}}(\boldsymbol{r})/\partial t = 0$)

$$\frac{\partial}{\partial t}\boldsymbol{j}(\boldsymbol{r},t) = -i\langle\Psi(t)|[\hat{\boldsymbol{j}}(\boldsymbol{r}), \hat{H}(t)]|\Psi(t)\rangle \tag{1.20}$$

$$\frac{\partial}{\partial t}\boldsymbol{j}'(\boldsymbol{r},t) = -i\langle\Psi'(t)|\hat{\boldsymbol{j}}(\boldsymbol{r}), \hat{H}'(t)]|\Psi'(t)\rangle. \tag{1.21}$$

Taking the difference between (1.20) and (1.21) at initial time, and since we take $\Psi = \Psi' = \Psi(t=0)$ at $t=0$, we arrive at

$$\begin{aligned}\frac{\partial}{\partial t}[\boldsymbol{j}(\boldsymbol{r},t) - \boldsymbol{j}'(\boldsymbol{r},t)]\Big|_{t=0} &= -i\langle\Psi(t=0)|[\hat{\boldsymbol{j}}(\boldsymbol{r}), \hat{H}(t=0) - \hat{H}'(t=0)]|\Psi(t=0)\rangle \\ &= n(\boldsymbol{r},t=0)\nabla[v_{ext}(\boldsymbol{r},t=0) - v'_{ext}(\boldsymbol{r},t=0)]\end{aligned} \tag{1.22}$$

with the last equality coming from the fact that the primed and unprimed Hamiltonians are identical with the exception of the external potentials (since the kinetic and the electron-electron operators are identical by definition of the Hamiltonians and their values are taken for the same wavefunction).

Equation (1.22) thus implies that if condition (1.16) is met for $k=0$, then

$$v_{ext}(\boldsymbol{r},t=0) - v'_{ext}(\boldsymbol{r},t=0) \neq 0, \tag{1.23}$$

with

$$v_{ext}(\boldsymbol{r},t=0) = v_{ext,0}(\boldsymbol{r}) \tag{1.24}$$

$$v'_{ext}(\boldsymbol{r},t=0) = v'_{ext,0}(\boldsymbol{r}), \tag{1.25}$$

and therefore, since the right-hand side of (1.22) doesn't vanish, the current-densities $\boldsymbol{j}$ and $\boldsymbol{j}'$ will differ infinitesimally later than $t=0$. If (1.16) is met only for an integer $k>0$, we apply the equation of motion another k times, leading us to

$$\Big(\frac{\partial}{\partial t}\Big)^{k+1}[\boldsymbol{j}(\boldsymbol{r},t) - \boldsymbol{j}'(\boldsymbol{r},t)]\Big|_{t=0} = -n(\boldsymbol{r},t=0)\nabla w_k(\boldsymbol{r}), \tag{1.26}$$

where

$$w_k(\boldsymbol{r}) = \Big(\frac{\partial}{\partial t}\Big)^k [v_{ext}(\boldsymbol{r},t) - v'_{ext}(\boldsymbol{r},t)]\Big|_{t=0} \\ = v_{ext,k}(\boldsymbol{r}) - v'_{ext,k}(\boldsymbol{r}), \tag{1.27}$$

and we get yet again that the currents are different infinitesimally after $t = 0$.

Now that a map from the density currents to the external potentials for a given initial-state has been established, we have to prove the same mapping but from the one-particle electronic density $n(\boldsymbol{r},t)$ to the current-densities. We do this again by proving that different current-densities mean that the particle densities themselves are different, and use that to connect $n(\boldsymbol{r},t)$ to the external potential. Beginning by taking the continuity equation which relates both quantities

$$\Big(\frac{\partial}{\partial t}\Big) n(\boldsymbol{r},t) = -\nabla \cdot \boldsymbol{j}(\boldsymbol{r},t), \tag{1.28}$$

taking its time derivative $(k+1)$ times at $t = 0$ and subtracting the resulting expressions for $n(\boldsymbol{r},t)$ and $n'(\boldsymbol{r},t)$, we get

$$\Big(\frac{\partial}{\partial t}\Big)^{k+2} [n(\boldsymbol{r},t) - n'(\boldsymbol{r},t)]\Big|_{t=0} = -\nabla \cdot \Big(\frac{\partial}{\partial t}\Big)^{k+1} [\boldsymbol{j}(\boldsymbol{r},t) - \boldsymbol{j}'(\boldsymbol{r},t)]\Big|_{t=0}, \tag{1.29}$$

which, after applying (1.22), reduces to

$$\Big(\frac{\partial}{\partial t}\Big)^{k+2} [n(\boldsymbol{r},t) - n'(\boldsymbol{r},t)]\Big|_{t=0} = \nabla \cdot [n(\boldsymbol{r},t=0)\nabla w_k(\boldsymbol{r})]. \tag{1.30}$$

It remains for us to show that if (1.16) holds, then the right-hand side of (1.27) doesn't vanish and different external potentials do in fact lead to different particle densities, which now due to the divergence operator is less trivial than before. To do so, we consider the following integral relationship (Green's integral theorem):

$$\int d^3r n(\boldsymbol{r},t=0)(\nabla w_k(\boldsymbol{r}))^2 = -\int d^3r w_k(\boldsymbol{r}) \nabla \cdot [n(\boldsymbol{r},t=0)\nabla w_k(\boldsymbol{r})] \\ + \oint d\boldsymbol{S} \cdot [n(\boldsymbol{r},t=0) w_k(\boldsymbol{r}) \nabla w_k(\boldsymbol{r})]. \tag{1.31}$$

For all physically reasonable potentials (ones that arise from normalizable external charge distributions, that do not diverge for large $|\boldsymbol{r}|$) the surface integral vanishes. Therefore, since the integrand function on the left-hand side of (1.30) is strictly non-negative and $w_k \neq 0$ by definition, we get that

$$\nabla \cdot [n(\boldsymbol{r},t=0)\nabla w_k(\boldsymbol{r})] \neq 0 \tag{1.32}$$

and thus prove the right-hand side of (1.30) doesn't vanish. This finishes the proof for the Runge-Gross theorem, showing how different external potentials for the same initial

wavefunction lead to different densities immediately after $t = 0$. Since by solving the time-dependent Schrödinger equation for a fixed initial state we have the map

$$\Psi(t = 0) : v_{ext}(\boldsymbol{r}, t) \rightarrow n(\boldsymbol{r}, t), \tag{1.33}$$

what the Runge-Gross theorem does is to show that for a certain set of conditions it can be inverted, thus allowing us to write

$$\Psi(t = 0) : v_{ext}(\boldsymbol{r}, t) \leftrightarrow n(\boldsymbol{r}, t). \tag{1.34}$$

There is therefore a one-to-one correspondence between the external potential and the time-dependent density.

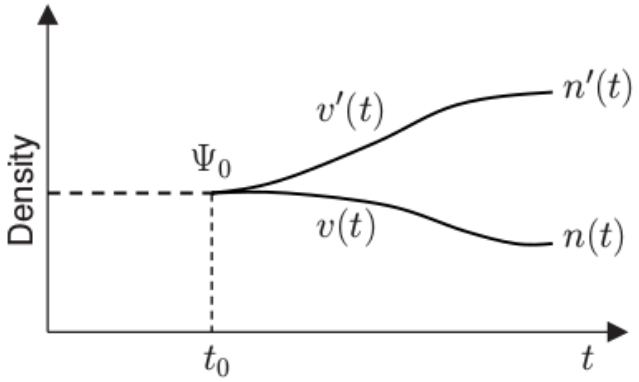

Figure 1.1: Illustration of the time evolution of the density when subjected to different time-dependent potentials [18]

An immediate consequence of the theorem is that both the Hamiltonian and the many-body wavefunction are functionals of the density and the initial state [1]. From this dependency, we get that *every* physical observable is a functional of the density and initial state:

$$O(t) = \langle \Psi[n, \Psi_0] | \hat{O}(t) | \Psi[n, \Psi_0] \rangle = O[n, \Psi_0](t). \tag{1.35}$$

As powerful as equation (1.35) is, since it tells us that we can in principle obtain any and every observable uniquely through $n(\boldsymbol{r}, t)$ and $|\Psi_0\rangle$, we would still like to use a scheme analogous to the Kohn-Sham one, due to the advantages it brings us already demonstrated in ground-state DFT. This is however not covered in the Runge-Gross theorem, and it thus needs to be proven, which is done using the van Leeuwen theorem [12].

The van Leeuwen theorem proves that (for additional conditions besides the ones for the Runge-Gross theorem, like the density being time analytic) the same $n(\boldsymbol{r}, t)$ can

be reproduced for two systems with differing electron-electron and external potentials, as well as initial states (on the condition that they yield the same density and its time derivative at $t = 0$). In the specific case where one system is the real, interacting one and the other is a non-interacting system, we get our desired Kohn-Sham approach in the time-dependent case. The question of whether or not this can be done for all cases and, if not, when can it be done, is called the non-interacting v-representability problem and is an open problem. Regarding this issue, the van Leeuwen theorem only assures that this system exists for the time-dependent part of the potential if it is time analytic and the initial state is compatible with the requirements mentioned above; whether or not this initial state exists is the ground-state non-interacting v-representability problem.

Another specific case of interest is the case where the interactions and initial states are the same for both systems. For this scenario, the van Leeuwen theorem reproduces the Runge-Gross theorem, i.e. that there is a one-to-one map between density and external potential, thus proving that the second is a special case of the first.

With this, we have all the fundamental basis to proceed to the time-dependent Kohn-Sham scheme.

1.2 Time-Dependent Kohn-Sham Equations

In order to get the time-dependent version of the Kohn-Sham equations, we assume that the non-interacting system mentioned in the previous section does exist and we do not run into the v-representability problem. Therefore, there exists an external potential (which we refer to as the Kohn-Sham potential) $v_s[n, \Psi_0, \Phi_0](\boldsymbol{r}, t)$, with $|\Psi_0\rangle$ the initial many-body state and $|\Phi_0\rangle$ the initial state of the non-interacting system, under which this fictitious system evolves and in a way that exactly reproduces the correct charge density $n(\boldsymbol{r}, t)$.

In many practical cases, like the linear-response regime, the functional dependence of v_s on the initial state can be dropped. This simplification arises when the system of interest is initially in its ground state. If that is the case, then through the Hohenberg-Kohn theorem of ground-state DFT (as long as $|\Psi_0\rangle$ and $|\Phi_0\rangle$ are non-degenerate ground-states) the initial states are functionals of the ground-state density $n_0(\boldsymbol{r})$ and therefore the Kohn-Sham potential is a functional only of that quantity.

When the time dependent potential is turned on, the system is forced to leave its ground-state. As such, instead of obeying the ground-state Kohn-Sham equations, it must obey their time-dependent version:

$$i\frac{\partial}{\partial t}\varphi_j(\boldsymbol{r}, t) = \left[-\frac{\nabla^2}{2} + v_s[n](\boldsymbol{r}, t) \right] \varphi_j(\boldsymbol{r}, t), \tag{1.36}$$

with φ_j the Kohn-Sham orbitals such that

$$\Phi_0(\boldsymbol{r}_1, \boldsymbol{r}_2, ..., \boldsymbol{r}_N, t) = \frac{1}{\sqrt{N!}} \begin{vmatrix} \varphi_i(\boldsymbol{r}_1, t) & \varphi_j(\boldsymbol{r}_1, t) & ... & \varphi_k(\boldsymbol{r}_2, t) \\ \varphi_i(\boldsymbol{r}_2, t) & \varphi_j(\boldsymbol{r}_2, t) & ... & \varphi_k(\boldsymbol{r}_2, t) \\ ... & ... & ... & ... \\ \varphi_i(\boldsymbol{r}_N, t) & \varphi_j(\boldsymbol{r}_N, t) & ... & \varphi_k(\boldsymbol{r}_N, t) \end{vmatrix}. \tag{1.37}$$

and obeying the initial-time condition $\varphi_j(\boldsymbol{r}, t = t_0) = \varphi_j^0(\boldsymbol{r})$, i.e corresponding to the ground-state Kohn-Sham orbitals. The time-dependent charge density is then given by

$$n(\boldsymbol{r}, t) = \sum_{j=1}^{N} |\varphi_j(\boldsymbol{r}, t)|^2. \tag{1.38}$$

The potential v_s that appears in (1.36) is the sum of three parts just like in the ground-state case:

$$v_s[n](\boldsymbol{r}, t) = v_{ext}(\boldsymbol{r}, t) + \int d^3r' \frac{n(\boldsymbol{r}', t)}{|\boldsymbol{r} - \boldsymbol{r}'|} + v_{xc}[n](\boldsymbol{r}, t), \tag{1.39}$$

with the first term being the time-dependent external potential, the second one the time-dependent Hartree potential and the third one the time-dependent exchange-correlation potential.

Equation (1.39) defines the exchange-correlation potential: it is the difference between the external potential of the non-interacting system v_s, which generates the same density $n(\boldsymbol{r}, t)$ as the interacting one by definition, and both the one from the interacting system v_{ext} and the time-dependent Hartree potential. If we know the initial state of our system, this will be the unknown functional that we need to approximate in TDDFT (if we need to calculate the initial state as well, then an approximation for the ground-state v_{xc} is also required, with the condition that they have to match at the instant the time-dependent part of v_{ext} is turned on).

1.3 Linear Response In TDDFT

Now that we have a Kohn-Sham scheme for TDDFT, we can move along to linear response and, in particular, the calculation of linear response functions.

Response functions describe the way a system changes when perturbed by an external source. Because these functions are non-local both in space and in time, TDDFT is a natural framework for their calculation (although there are other frameworks who are equally valid for that purpose) [15]. They are also of extreme importance since it is through them that we can calculate very important observables, such as neutral (that conserve number of electrons) excitation energies (as we will see soon) and optical spectra [1].

If we consider our interacting system of interest to be initially in its ground state, and that at $t = t_0$ a time dependent perturbation is turned on, we can write our external potential as

$$v_{ext}(\boldsymbol{r},t) = v_{ext}(\boldsymbol{r}) + \delta v_{ext}(\boldsymbol{r},t)\Theta(t-t_0), \tag{1.40}$$

with the Heaviside function Θ guaranteeing that the time-dependent part of the potential is only turned on at $t = t_0$. The system will therefore be forced to leave the ground-state by $\delta v_{ext}(\boldsymbol{r},t)$ as soon as it is turned on. This means that both until $t = t_0$, via the Hohenberg-Kohn theorem, and after $t = t_0$, via the Runge-Gross theorem, we guarantee a one-to-one map between the time-dependent density and v_{ext}, which shows that we can write $n(\boldsymbol{r},t)$ as a functional of $v_{ext}(\boldsymbol{r},t)$ exclusively, i.e. $n(\boldsymbol{r},t) = n[v_{ext}](\boldsymbol{r},t)$.

If we consider $\delta v_{ext}(\boldsymbol{r},t)$ to be a weak time-analytic perturbation to the system, we can then write $n(\boldsymbol{r},t)$ as a Taylor series relative to $\delta v_{ext}(\boldsymbol{r},t)$. We therefore write

$$n(\boldsymbol{r},t) = n_0(\boldsymbol{r}) + n_1(\boldsymbol{r},t) + n_2(\boldsymbol{r},t) + ..., \tag{1.41}$$

$n_0(\boldsymbol{r})$ being the ground-state density, with the guarantee that higher-order terms are smaller than lower-order ones and therefore $n(\boldsymbol{r},t)$ does not diverge.

In this chapter we are concerned with linear response, which means we are dealing with the first time-dependent correction to the ground-state density $n_1(\boldsymbol{r},t)$. This correction can be written as

$$n_1(\boldsymbol{r},t) = \int dt' \int d^3r' \chi(\boldsymbol{r},t,\boldsymbol{r}',t')\delta v_{ext}(\boldsymbol{r}',t'). \tag{1.42}$$

Here,

$$\chi(\boldsymbol{r},t,\boldsymbol{r}',t') = \left.\frac{\delta n(\boldsymbol{r},t)}{\delta v_{ext}(\boldsymbol{r}',t')}\right|_{v_{ext}(\boldsymbol{r})} \tag{1.43}$$

and it corresponds to the density-density linear response function; it represents the system's first-order response to the external time-dependent perturbation, and it is calculated at the initial time-independent external potential $v_{ext}(\boldsymbol{r})$ as it is a characteristic of the system and not of the perturbation.

From ordinary time-dependent perturbation theory relative to v_{ext} [15] we can write

$$\chi(\boldsymbol{r},t,\boldsymbol{r}',t') = -i\Theta(t-t')\left\langle\Psi_0\right|\left[\hat{n}_{H_{gs}(\boldsymbol{r},t)}, \hat{n}_{H_{gs}(\boldsymbol{r}',t')}\right]\left|\Psi_0\right\rangle \tag{1.44}$$

,

with $\hat{n}$ the density-operator in the interaction picture and H_{gs} the ground-state hamiltonian. By inserting an identity in the form of a completeness of interacting state, i.e. inserting $\sum_\lambda |\Psi_\lambda\rangle\langle\Psi_\lambda|$, we can Fourier transform (1.44) with respect to $t - t'$ to obtain the expression for χ in the Lehmann representation:

$$\chi(\boldsymbol{r},\boldsymbol{r}',\omega) = \lim_{\eta\to 0^+}\sum_\lambda\left[\frac{\langle\Psi_0|\hat{n}(\boldsymbol{r})|\Psi_\lambda\rangle\langle\Psi_\lambda|\hat{n}(\boldsymbol{r}')|\Psi_0\rangle}{\omega-(E_\lambda-E_0)+i\eta} - \frac{\langle\Psi_0|\hat{n}(\boldsymbol{r}')|\Psi_\lambda\rangle\langle\Psi_\lambda|\hat{n}(\boldsymbol{r})|\Psi_0\rangle}{\omega+(E_\lambda-E_0)+i\eta}\right], \tag{1.45}$$

Here, the sum is for all excited states, Ψ_0 corresponds to the ground-state of the interacting system, Ψ_λ to an excited state, and the difference $E_\lambda - E_0$ corresponds to the excitation energy from the ground-state to the excited state λ. This is an important feature of the density-density linear response function: its poles are the exact excitation energies for neutral excitations.

Calculating this function within the interacting system is a very difficult task, as it requires the knowledge of the many-body wavefunction which is what we have been avoiding from the beginning. However, we have the formal justification to calculate it through the Kohn-Sham scheme, which makes the calculation easier in principle.

In the Kohn-Sham scheme, due to the external potential in the case of the non-interacting system being $v_s[n](\boldsymbol{r}, t)$ given by (1.39), and since $n(\boldsymbol{r}, t)$ (as shown previously) can be calculated exactly in it, we get that the first-order perturbation to the density $n_1(\boldsymbol{r}, t)$ is given by

$$n_1(\boldsymbol{r}, t) = \int dt' \int d^3r' \chi_s(\boldsymbol{r}, t, \boldsymbol{r}', t') \delta v_s(\boldsymbol{r}', t'), \tag{1.46}$$

where δv_s is the analogue to δv_{ext} from (1.40) in the Kohn-Sham scheme and χ_s is the density-density response function for the non-interacting system:

$$\chi_s(\boldsymbol{r}, t, \boldsymbol{r}', t') = \left. \frac{\delta n(\boldsymbol{r}, t)}{\delta v_s(\boldsymbol{r}', t')} \right|_{v_s[n_0]}. \tag{1.47}$$

Writing χ_s in the Lehmann representation and in the basis set of the Kohn-Sham orbitals, we arrive at

$$\chi_s(\boldsymbol{r}, \boldsymbol{r}', \omega) = \lim_{\eta \to 0^+} \sum_{j,k} (f_k - f_j) \frac{\varphi_k^{(0)*}(\boldsymbol{r}) \varphi_j^{(0)}(\boldsymbol{r}) \varphi_j^{(0)*}(\boldsymbol{r}') \varphi_k^{(0)}(\boldsymbol{r}')}{\omega - (\epsilon_j - \epsilon_k) + i\eta}, \tag{1.48}$$

where f_j and f_k are occupation numbers and $\epsilon_j - \epsilon_k$ are the Kohn-Sham excitation energies. These energy differences, unlike the ones in (1.45), don't correspond to the real excitation energies, which reinforces the fact that χ_s is not in fact the same as χ from (1.43). This is obvious from the fact that if that were the case, δv_s would be equal to δv_{ext}.

In order to get the interacting system's response function from the Kohn-Sham scheme, we begin by writing out δv_s explicitly from (1.39):

$$\delta v_s(\boldsymbol{r}, t) = \delta v_{ext}(\boldsymbol{r}, t) + \delta v_H(\boldsymbol{r}, t) + \delta v_{xc}[n](\boldsymbol{r}, t), \tag{1.49}$$

with

$$\delta v_H(\boldsymbol{r}, t) = \int d^3r' \frac{n_1(\boldsymbol{r}', t)}{|\boldsymbol{r} - \boldsymbol{r}'|}. \tag{1.50}$$

The last term of (1.49) is the first-order change in the exchange-correlation potential, and in order to write it explicitly we do a Taylor expansion on the functional and define the xc kernel f_{xc} as

$$f_{xc}(\boldsymbol{r},t,\boldsymbol{r}',t') = \left.\frac{\delta v_{xc}[n](\boldsymbol{r},t)}{\delta n(\boldsymbol{r}',t')}\right|_{n=n_0}. \tag{1.51}$$

This leads us to

$$\delta v_{xc}[n](\boldsymbol{r},t) = \int dt' \int d^3r' f_{xc}(\boldsymbol{r},t,\boldsymbol{r}',t') n_1(\boldsymbol{r}',t'), \tag{1.52}$$

and, therefore, we get for δv_s:

$$\delta v_s(\boldsymbol{r},t) = \delta v_{ext}(\boldsymbol{r},t) + \int d^3r' \frac{n_1(\boldsymbol{r}',t)}{|\boldsymbol{r}-\boldsymbol{r}'|} + \int dt' \int d^3r' f_{xc}(\boldsymbol{r},t,\boldsymbol{r}',t') n_1(\boldsymbol{r}',t'). \tag{1.53}$$

By substituting (1.53) into (1.46) and setting it equal to (1.42), we get a Dyson-like equation for the linear response function χ. Defining the Hartree-xc kernel for convenience as

$$f_{Hxc} = \frac{\delta(t-t')}{|\boldsymbol{r}-\boldsymbol{r}'|} + f_{xc}(\boldsymbol{r},t,\boldsymbol{r}',t'), \tag{1.54}$$

and after some algebra, we arrive at

$$\begin{aligned}\chi(\boldsymbol{r},t,\boldsymbol{r}',t') =& \chi_s(\boldsymbol{r},t,\boldsymbol{r}',t') + \\ &+ \int dt_1 \int d^3r_1 \int dt_2 \int d^3r_2\, \chi_s(\boldsymbol{r},t,\boldsymbol{r}_1,t_1) f_{Hxc}(\boldsymbol{r}_1,t_1,\boldsymbol{r}_2,t_2) \chi(\boldsymbol{r}_2,t_2,\boldsymbol{r}',t').\end{aligned} \tag{1.55}$$

It is this Dyson-type equation for the linear response function (usually in frequency space) that allows us to calculate observables of the interacting system like the aforementioned excitation energies.

Even though equation (1.55) is exact, in practice we have to approximate χ_s and f_{Hxc} since we do not know the exact ground-state xc-potential and xc-kernel. The quality of the calculated χ is thus determined by how good the approximations used are, making this task a crucial one since if a good approximation cannot be reached, then this whole process has no practical value (at least not for the purposes mentioned in this chapter).

One of the most common approximations used for the xc-kernel is the adiabatic approximation, meaning that we remove all memory dependence from f_{xc}. While in general, as mentioned previously, the xc-potential is a functional of the density, the initial interacting state $|\Psi_0\rangle$ and the initial non-interacting state $|\Phi_0\rangle$, for our purposes of linear response it is a functional exclusively of the density since we take our system to be initially in its ground-state. By making an adiabatic approximation to the xc-kernel, we are effectively removing its memory dependence by replacing the time-dependent $v_{xc}[n](\boldsymbol{r},t)$ at every instant t by the ground-state v_{xc} of a system with density $n(\boldsymbol{r},t)$:

$$v^{adia}[n](\boldsymbol{r},t) = v_{xc}^{(0)}[n(\boldsymbol{r},t)](\boldsymbol{r}). \tag{1.56}$$

This in turn leads to a static version of the xc-kernel, which can be written in a simple form as:

$$f_{xc}(\boldsymbol{r},\boldsymbol{r}') = \frac{\delta v_{xc}^{(0)}[n_0](\boldsymbol{r})}{\delta n_0(\boldsymbol{r}')} = \frac{\delta E_{xc}[n_0]}{\delta n_0(\boldsymbol{r})\delta n_0(\boldsymbol{r}')}. \tag{1.57}$$

The adiabatic approximation is a good one from a fundamental point-of-view when the time-dependence on the external potential is slowly-varying and the system begins in the ground state (since this allows for the initial state dependence to be removed). An example of one of these adiabatic approximations is the ALDA, which is local in both space and time and is perhaps the simplest approximation for a non-zero xc-kernel.

An example of a linear response function is the first-order dynamic polarizability $\alpha(\omega)$ of an atom or a molecule, the system's dipole moment μ's linear response when perturbed by an external dipolar electric field $\mathcal{E}$:

$$\alpha_{ij}(\omega) = \frac{\partial \mu_i(\omega)}{\partial \mathcal{E}_j(\omega)}. \tag{1.58}$$

However, in order to calculate this quantity, we need to use a method based on perturbation theory, like the Sternheimer equations. This discussion will be done in a later chapter.

1.4 Higher-Order Response

The same thought-process applied to obtain the first-order density-density response in the previous chapter can be used in order to get higher-order response functions, like the second-order one which allows us to calculate a correction to the ground-state density like $n_2(\boldsymbol{r},t)$ from (1.41). From here on out we will assume implicit integration on bar-variables in order to simplify expressions, e.g. $\int f(r,r')g(r',r'')dr' = f(r,\bar{r'})g(\bar{r'},r'')$.

In order to obtain the second-order density-density response function, let us begin by considering the time-dependent part of the external potential can be written as a sum of a linear and a quadratic component (if such a component exists), i.e. that

$$v_{ext}(\boldsymbol{r},t) = v_{ext}(\boldsymbol{r}) + \delta v_{ext}^{(1)}(\boldsymbol{r},t) + \delta v_{ext}^{(2)}(\boldsymbol{r},t). \tag{1.59}$$

In linear response we had that the first-order change in density $n_1(\boldsymbol{r},t)$ is a result of first-order perturbations by the time-dependent potential, which is simply $\delta v_{ext}^{(1)}(\boldsymbol{r},t)$. For $n_2(\boldsymbol{r},t)$ however, it is the result of second-order perturbations, which are now not only due to $\delta v_{ext}^{(2)}(\boldsymbol{r},t)$ but also due to $\delta v_{ext}^{(1)}(\boldsymbol{r},t)\delta v_{ext}^{(1)}(\boldsymbol{r}',t')$, as this is also second-order in the field strength. In the time-domain we thus get

$$n_2(\boldsymbol{r},t) = \frac{1}{2}\chi^{(2)}(\boldsymbol{r},t,\bar{\boldsymbol{r}'},\bar{t'},\bar{\boldsymbol{r}''},\bar{t''})\delta v_{ext}^{(1)}(\bar{\boldsymbol{r}'},\bar{t'})\delta v_{ext}^{(1)}(\bar{\boldsymbol{r}''},\bar{t''}) + \chi^{(1)}(\boldsymbol{r},t,\bar{\boldsymbol{r}'},\bar{t'})\delta v_{ext}^{(2)}(\bar{\boldsymbol{r}'},\bar{t'}). \tag{1.60}$$

As for the Kohn-Sham second-order response, we get

$$\begin{aligned} n_2(\boldsymbol{r},t) =& \frac{1}{2}\chi_s^{(2)}(\boldsymbol{r},t,\bar{\boldsymbol{r}'},\bar{t'},\bar{\boldsymbol{r}''},\bar{t''})\delta v_{ext}^{(1)}(\bar{\boldsymbol{r}'},\bar{t'})\delta v_{ext}^{(1)}(\bar{\boldsymbol{r}''},\bar{t''}) + \\ &+\chi_s^{(1)}(\boldsymbol{r},t,\bar{\boldsymbol{r}'},\bar{t'})\delta v_{ext}^{(2)}(\bar{\boldsymbol{r}'},\bar{t'}) + \\ &+\frac{1}{2}\chi_s^{(1)}(\boldsymbol{r},t,\bar{\boldsymbol{r}'},\bar{t'})k_{xc}(\bar{\boldsymbol{r}'},\bar{t'},\bar{\boldsymbol{r}''},\bar{t''},\bar{\boldsymbol{r}'''},\bar{t'''})n_1(\bar{\boldsymbol{r}''},\bar{t''})n_1(\bar{\boldsymbol{r}'''},\bar{t'''}) + \\ &+\chi_s^{(1)}(\boldsymbol{r},t,\bar{\boldsymbol{r}'},\bar{t'})f_{Hxc}(\bar{\boldsymbol{r}'},\bar{t'},\bar{\boldsymbol{r}''},\bar{t''})n_2(\bar{\boldsymbol{r}''},\bar{t''}), \end{aligned} \tag{1.61}$$

with f_{Hxc} as defined in (1.43) and with k_{xc} the second-order xc-kernel:

$$k_{xc}(\boldsymbol{r}',t',\boldsymbol{r}'',t'',\boldsymbol{r}''',t''') = \left.\frac{\delta^2 v_{xc}[n](\boldsymbol{r}',t')}{\delta n(\boldsymbol{r}'',t'')\delta n(\boldsymbol{r}''',t''')}\right|_{n=n_0}. \tag{1.62}$$

As we can see in (1.61), in order to calculate second-order response we need the first-order calculation (as well as the ground-state). This is a characteristic of response functions: they form a hierarchy where the higher order response functions depend on lower order ones and thus require them to be calculated beforehand.

An example of a second-order response function would be the first hyperpolarizability, the second-order version of the change in dipole moment mentioned in the previous chapter:

$$\beta_{ijk}(\omega = \omega_1 + \omega_2) = \frac{\partial^2 \mu_i(\omega)}{\partial \mathcal{E}_j(\omega_1)\mathcal{E}_k(\omega_2)^2} \tag{1.63}$$

Again, in order to calculate this quantity we need to use a method like the Sternheimer one. This is the next chapter's goal.

1.5 The Sternheimer Method

In order to see how we can calculate response-functions of various orders using the Sternheimer method, we begin by again considering our time-dependent external potential is a weak one and that it depends on a frequency ω. Then, we can write it as

$$v_{ext}(\boldsymbol{r},t) = \lambda v_{ext}^{+\omega}(\boldsymbol{r})e^{+i\omega t} + \lambda v_{ext}^{-\omega}(\boldsymbol{r})e^{-i\omega t}, \tag{1.64}$$

with λ the strength of the perturbation.

Our goal with this method is to take advantage of the fact that, due to the potential being weak, we can take the time-dependent Kohn-Sham equations

$$i\frac{\partial}{\partial t}\varphi_j(\boldsymbol{r},t) = \hat{H}_{KS}[n](\boldsymbol{r},t)\varphi_j, \tag{1.65}$$

with

$$\hat{H}_{KS}[n](\boldsymbol{r},t) = -\frac{\nabla^2}{2} + v_s[n](\boldsymbol{r},t) \tag{1.66}$$

and with v_s defined by (1.39), and do a perturbative expansion on both φ and $\hat{H}_{KS}$ with respect to λ. By doing this and setting members with the same perturbation strength equal, we hope to obtain a set of equations that allow us to calculate the corrections to the orbitals and therefore the various orders of the density response.

Considering, for simplicity, that we are working within the adiabatic approximation, and that our system is spin-unpolarized, has integer occupations and the ground-state Kohn-Sham orbitals are real, we begin by writing our Kohn-Sham states and Hamiltonian in a perturbative expansion:

$$\varphi_j(\boldsymbol{r},t) = \varphi_j^{(0)}(\boldsymbol{r},t) + \lambda\varphi_j^{(1)}(\boldsymbol{r},t) + \lambda^2\varphi_j^{(2)}(\boldsymbol{r},t) + ... \tag{1.67}$$

$$\hat{H}_{KS}[n](\boldsymbol{r},t) = \hat{H}_{KS}^{(0)}[n^{(0)}](\boldsymbol{r},t) + \lambda v_{ext}^{(1)}(\boldsymbol{r},t) + \lambda\hat{H}_{KS}^{(1)}[n](\boldsymbol{r},t) + \lambda^2 v_{ext}^{(2)}(\boldsymbol{r},t) + \lambda^2\hat{H}_{KS}^{(2)}[n](\boldsymbol{r},t) + ... \tag{1.68}$$

Here $H_{KS}^{(0)}$ is the ground-state Hamiltonian, which means we can remove its time-dependence and write it simply as $H_{KS}^{(0)}(\boldsymbol{r})$. The $H_{KS}^{(k)}$ are the k-th order response Hamiltonians, and they reflect the fact that when the system is perturbed by $v_{ext}(\boldsymbol{r},t)$ the system's internal potentials (Hartree and xc) are affected and change due to it.

Setting the terms of (1.67) and (1.68) with the same order λ equal, we get a time-dependent Kohn-Sham equation for every order of the response. For example, for zeroth and first-order we get

$$i\frac{\partial}{\partial t}\varphi_j^{(0)}(\boldsymbol{r},t) = \hat{H}_{KS}^{(0)}[n^{(0)}](\boldsymbol{r},t)\varphi_j^{(0)}(\boldsymbol{r},t) \tag{1.69}$$

and

$$i\frac{\partial}{\partial t}\varphi_j^{(1)}(\boldsymbol{r},t) = \hat{H}_{KS}^{(0)}[n^{(0)}](\boldsymbol{r},t)\varphi_j^{(1)}(\boldsymbol{r},t) + \Big\{\hat{H}_{KS}^{(1)}[n](\boldsymbol{r},t) + v_{ext}^{(1)}(\boldsymbol{r},t)\Big\}\varphi_j^{(1)}(\boldsymbol{r},t) \tag{1.70}$$

respectively.

If we assume that in our case we only have one frequency dependence ω in the potential as just described, we can write it as in (1.64) and $\varphi^{(1)}$'s frequency dependence will be on just ω as well. This means our first-order wavefunction can be written as

$$\varphi(\boldsymbol{r},t) = e^{-i\epsilon^{(0)}t}\Big\{\varphi^{(0)}(\boldsymbol{r}) + \lambda\Big[\varphi_{+\omega}^{(1)}(\boldsymbol{r})e^{+i\omega t} + \varphi_{-\omega}^{(1)}(\boldsymbol{r})e^{-i\omega t}\Big]\Big\} + \mathcal{O}(\lambda^2) + ..., \tag{1.71}$$

where we approximate the time-dependence on the wavefunction due to the Hamiltonian as $e^{-iE(t)} = e^{-i\epsilon^{(0)}t - i\lambda\Delta\epsilon^{(1)}(t)}$, with

$$\Delta\epsilon^{(1)}[n](t) = \int_{-\infty}^{t} dt \langle\varphi^{(0)}|\hat{H}^{(1)}_{KS}[n](t) + v^{(1)}_{ext}(t)|\varphi^{(0)}\rangle. \tag{1.72}$$

This allows us to write $\varphi^{(1)}_{\pm\omega}$ with only a spatial dependence while keeping it orthogonal to $\varphi^{(0)}$.

Substituting (1.71) in (1.65), we obtain for the l.h.s.:

$$\begin{aligned} i\frac{\partial}{\partial t}\varphi_j(\boldsymbol{r},t) = e^{-i\epsilon^{(0)}t - i\lambda\Delta\epsilon^{(1)}(t)}\Bigg\{\left[\epsilon^{(0)}_j + \lambda\frac{\partial}{\partial t}\Delta\epsilon^{(1)}_j(t)\right]\varphi^{(0)}_j(\boldsymbol{r}) + \\ + \lambda(\epsilon^{(0)}_j - \omega)\varphi^{(1)}_{j,+\omega}(\boldsymbol{r})e^{i\omega t} + \lambda(\epsilon^{(0)}_j + \omega)\varphi^{(1)}_{j,-\omega}(\boldsymbol{r})e^{-i\omega t}\Bigg\} + \mathcal{O}(\lambda^2). \end{aligned} \tag{1.73}$$

As for the r.h.s., we get:

$$\begin{aligned} \hat{H}_{KS}[n](\boldsymbol{r},t)\varphi_j(\boldsymbol{r},t) = e^{-i\epsilon^{(0)}t - i\lambda\Delta\epsilon^{(1)}(t)}\Bigg\{\hat{H}^{(0)}_{KS}[n^{(0)}](\boldsymbol{r})\varphi^{(0)}_j(\boldsymbol{r}) + \lambda\hat{H}^{(0)}_{KS}[n^{(0)}](\boldsymbol{r})\times \\ \left[\varphi^{(1)}_{j,+\omega}(\boldsymbol{r})e^{i\omega t} + \varphi^{(1)}_{j,-\omega}(\boldsymbol{r})e^{-i\omega t}\right] + \lambda\left[\int d^3r' f_{Hxc}[n^{(0)}](\boldsymbol{r},\boldsymbol{r}')n^{(1)}(\boldsymbol{r}',t) + v^{(1)}_{ext}(\boldsymbol{r},t)\right]\varphi^{(0)}_j(\boldsymbol{r})\Bigg\} + \mathcal{O}(\lambda^2) \end{aligned} \tag{1.74}$$

In order to write this equation in terms of the $\varphi^{(0)}_j$ and $\varphi^{(1)}_j$ we need to know the time-dependent ground-state and first-order response densities. Using

$$n(\boldsymbol{r},t) = \sum_j n_j|\varphi_j(\boldsymbol{r},t)|^2 \tag{1.75}$$

and replacing φ_j with (1.67), we get

$$n(\boldsymbol{r},t) = \sum_j n_j\Big\{\left|\varphi^{(0)}_j(\boldsymbol{r},t)\right|^2 + \lambda\Big[\varphi^{(0)*}_j(\boldsymbol{r},t)\varphi^{(1)}_j(\boldsymbol{r},t) + \varphi^{(1)*}_j(\boldsymbol{r},t)\varphi^{(0)}_j(\boldsymbol{r},t)\Big] + \mathcal{O}(\lambda^2) + ...\Big\}. \tag{1.76}$$

Now using the simplified notation

$$n^{(1)}_{\pm\omega}(\boldsymbol{r},t) = \sum_j n_j\Big\{\varphi^{(0)*}_j(\boldsymbol{r})\varphi^{(1)}_{j,\pm\omega}(\boldsymbol{r}) + \varphi^{(1)*}_{j,\mp\omega}(\boldsymbol{r})\varphi^{(0)}_j(\boldsymbol{r})\Big\}e^{\pm i\omega t}, \tag{1.77}$$

$$v^{(1)}_{Hxc,\pm\omega}e^{\pm i\omega t} = \int d^3r' f_{Hxc}[n^{(0)}](\boldsymbol{r},\boldsymbol{r}')n^{(1)}_{\pm\omega}(\boldsymbol{r}',t), \tag{1.78}$$

taking the Fourier transform of $\frac{\partial}{\partial t}\Delta\epsilon_j^{(1)}(t)$

$$\epsilon_{j,\pm\omega}^{(1)} = \langle\varphi_j^{(0)}|v_{Hxc,\pm\omega}^{(1)} + v_{ext,\pm\omega}^{(1)}|\varphi^{(0)}\rangle, \tag{1.79}$$

and gathering terms proportional to the exponentials, we finally arrive to:

$$(\hat{H}_{KS}^{(0)} - \epsilon_j^{(0)} \pm \omega)\varphi_{j,\pm\omega}^{(1)} = -(v_{Hxc,\pm\omega}^{(1)} + v_{ext,\pm\omega}^{(1)} - \epsilon_{j,\pm\omega}^{(1)})\varphi_j^{(0)} \tag{1.80}$$

Equation (1.80) comprises a set of non-linear equations that must be solved self-consistently, as $v_{Hxc,\pm\omega}^{(1)}$ depends on $n_{\pm\omega}^{(1)}$ and therefore on $\varphi_{j,\pm\omega}^{(1)}$.

We can simplify the calculation required by adding a projector to the unoccupied space $\hat{P}_{unocc}$, obtaining:

$$(\hat{H}_{KS}^{(0)} - \epsilon_j^{(0)} \pm \omega + i\eta)\varphi_{j,\pm\omega}^{(1)} = -\hat{P}_{unocc}(v_{Hxc,\pm\omega}^{(1)} + v_{ext,\pm\omega}^{(1)})\varphi_j^{(0)} \tag{1.81}$$

The additional term $i\eta$ serves as regulator and corresponds to introducing an artificial lifetime to v_{ext} and $\varphi_j^{(1)}$ that forces the system to return to the ground-state after a certain amount of time and has the effect of both removing singularities from (1.80) and stopping the response from becoming infinite at resonance frequencies.

The projector added in (1.81) is also very important. Since from perturbation theory we have

$$|\varphi_j^{(0)}|^2 = 1 \tag{1.82}$$

$$\begin{aligned}(\varphi_j^{(0)*} + \lambda\varphi_j^{(1)*})(\varphi_j^{(0)} + \lambda\varphi_j^{(1)}) = 1 \\ \Leftrightarrow |\varphi_j^{(0)}|^2 + \lambda\varphi_j^{(1)*}\varphi_j^{(0)} + \lambda\varphi_j^{(0)*}\varphi_j^{(1)} + \lambda^2|\varphi_j^{(1)*}| = 1 \\ \varphi_j^{(1)*}\varphi_j^{(0)} + \varphi_j^{(0)*}\varphi_j^{(1)} = 0.\end{aligned} \tag{1.83}$$

This means that in the subspace of the occupied $\varphi_j^{(0)}$, the components of $\varphi_j^{(1)}$ cancel out and therefore do not contribute to (1.77). This is equivalent to saying we are only interested in response orbitals that do not include the ground-state orbitals in them, i.e. we only want the *variation* relative to these orbitals. The projector therefore avoids doing these calculations, while also removing the $\epsilon_j^{(1)}$'s as they were included in order to orthogonalize the $\varphi_j^{(1)}$'s with respect to the $\varphi_j^{(0)}$'s, which the projector now takes care of.

The Sternheimer equation, together with the $2n+1$ theorem [5], are what allows us to calculate hyperpolarizabilities in an efficient way. The Sternheimer equation has the very useful characteristic of not needing the explicit calculation of a large number of unoccupied states in order to work, as it relies on the subspace of occupied ground-state Kohn-Sham orbitals, in contrast to other methods that might rely on an infinite sum over states. On the other hand the $2n+1$ theorem shows that the $2n+1$'st derivative of the total energy depends only on the solution of the n-order Sternheimer equation. In

the case of the first hyperpolarizability, which is the third-order derivative of the total energy with respect to the perturbing electric field, we only need to solve the first-order Sternheimer equation and obtain $\varphi_j^{(1)}$. Its expression is then given by

$$\beta = \sum_j^{occ} \langle \varphi_j^{(1)} | \hat{H}^{(1)} - \epsilon_j^{(1)} | \varphi_j^{(1)} \rangle + \langle \varphi_j^{(0)} | v_{ext}^{(2)} | \varphi_j^{(1)} \rangle + \langle \varphi_j^{(1)} | v_{ext}^{(2)} | \varphi_j^{(0)} \rangle + \langle \varphi_j^{(0)} | v_{ext}^{(3)} | \varphi_j^{(0)} \rangle + \\ + \frac{1}{6} k_{xc}(\bar{\boldsymbol{r}}, \bar{\boldsymbol{r}}', \bar{\boldsymbol{r}}'') n_1(\bar{\boldsymbol{r}}) n_1(\bar{\boldsymbol{r}}') n_1(\bar{\boldsymbol{r}}''), \tag{1.84}$$

where k_{xc} is (1.62) in the adiabatic approximation, $\hat{H}^{(1)} = v_{ext}^{(1)} + f_{Hxc}$ with f_{Hxc} given by (1.54) and f_{xc} by (1.57) and where $\epsilon_j^{(1)} = \langle \varphi_j^{(0)} | \hat{H}^{(1)} | \varphi_j^{(0)} \rangle$. Eq. (1.84) is the expression that will be used from now on in order to calculate hyperpolarizabilities.

Chapter 2

Genetic Algorithms

Genetic algorithms are a subset of evolutionary algorithms that attempt to mimic natural selection in order to solve optimization problems. In these kinds of algorithms the goal is to start from an initial set of individuals (a population) that we represent as a string of numbers (genes), and that have a given fitness associated to them that depends on these numbers and their order on the string, and to evolve it in such a way that this fitness is minimized or maximized (depending on the problem in hand).

This evolution is to be done iteratively, where in between generations the current population is subjected to a selection process where a subset of individuals is selected based on their fitness to reproduce and generate the next generation's population. The evolution is then stopped when either a certain predefined condition is achieved, like a maximum number of generations being hit, or the fitness of the individuals plateaus, and therefore no significant improvement is obtained by continuing with this process.

A number of operators can be used in order to improve and diversify each new generation of individuals relative to the previous one. Of these, the two most common ones are the crossover and mutation operations.

After the selection process occurs, those individuals that were selected due to their fitness are now subject to a process where two or more of them "breed", forming "child" individuals that are now part of a new generation (either together with the set of "parents" that generated them or just other "children", depending on the choice of recombination). It is to this breeding process that combines the information of two of the current population's fittest individuals in order to generate offspring that is called crossover. This attempts to imitate the way reproduction works in nature, with its effect being that it generates new individuals who will tend to increase (in the case of a maximization problem) the population's average fitness, moving it towards the goal of an optimal solution.

The mutation operation comes after crossover is done, and it consists on choosing random individuals from the newly formed generation population (including parents if those remain) and altering a set of its genes according to some predefined operation (e.g. turning each gene chosen to be mutated into their symmetric). This ensures more diversity in the population as it can not only allow the set of possible individuals to be

larger than the set of possible combinations of genes existing in the initial population, but also stops the system from losing diversity due to evolving in such a way that newer generations are too alike the older ones. The probability of a given individual being mutated is therefore a very important parameter for genetic algorithms: a too low mutation probability will lead to the aforementioned problems, while a too high one may lead to overly random newer generations (although this might not be an issue depending on the problem).

The problem of being tuned to the right value is, however, not exclusive to the mutation probability. If it is the case that crossover is probability reliant (e.g. if new generations are built by pairing individuals and then having a certain probability to either mate them or leave them as they were), then that is also an important parameter to adjust as it can have an effect on how much diversity of individuals is generated before convergence. Another important parameter to tune is the initial population size, as too small of a population can lead to not enough genetic diversity and therefore less optimal solutions. These are however all problem dependent and therefore there is not always a clear indication on what the correct values for each parameter are without testing.

As an example, let us consider we have two individuals A and B of length 5 that we represent as A = (1,0,1,0,1) and B = (0,1,0,1,0) that have passed the process of selection. Let us also consider that our crossover operator consists on selecting two individuals and a gene position and then switching the corresponding gene between them, and that our mutation operator has a chance for each individual to select a gene position and doing a bit-flip on the corresponding gene, i.e. if the gene is a 0 it is changed to a 1 and vice-versa. If A and B are selected as a pair for crossover and, for example, gene position 1 is selected in the crossover operator, the two individuals will produce the offspring A' = (0,0,1,0,1) and B' = (1,1,0,1,0) as a result.

Let us now suppose that only A' is selected for mutation and B' is left unchanged, with the mutation operator choosing gene position 4. The bit-flip then changes A' into (0,0,1,1,1), while B' remains written as (1,1,0,1,0). It is this A' and B' that are the offspring that will now be part of the next generation's population, and will again be subjected to the selection process, as well as the crossover and mutation operations in case they survive again.

Chapter 3

State Of The Art

The hyperpolarizability is an important quantity from a technological point of view, as systems with high values of β are often desired in order to improve the efficiency of certain processes. An example for this is the case of second-harmonic generation (also known as frequency doubling), a non-linear optical process with applications like the conversion of common 1064 nm laser beams into higher energy 532 nm ones. The importance of the second-order response in frequency doubling is easily seen by Fourier transforming (1.60), leading us to

$$n_2(r,\omega) = \frac{1}{2}\delta(\omega - \bar{\omega'} - \bar{\omega''})\chi^{(2)}(\boldsymbol{r},\omega,\bar{\boldsymbol{r}'},\bar{\omega'},\bar{\boldsymbol{r}''},\bar{\omega''})\delta v_{ext}^{(1)}(\bar{\boldsymbol{r}'},\bar{\omega'})\delta v_{ext}^{(1)}(\bar{\boldsymbol{r}''},\bar{\omega''}) + \chi^{(1)}(\boldsymbol{r},\omega,\bar{\boldsymbol{r}'},\bar{\omega'})\delta v_{ext}^{(2)}(\bar{\boldsymbol{r}'},\bar{\omega'}). \tag{3.1}$$

We can see from (3.1) that the second-order response function (the first hyperpolarizability in our case) will mix the two field frequencies ω' and ω'' and generate a third one that will be the frequency of the density response, with energy being conserved as expressed by $\delta(\omega - \bar{\omega'} - \bar{\omega''})$. In case the field has a single frequency ω (and is, therefore, monochromatic) like the case of 1064 nm laser beams, a non-zero $\chi^{(2)}$ will generate a response with frequency 2ω, effectively doubling the frequency (and, consequently, the energy) of the initial field. Since the response field with doubled frequency is proportional to $\chi^{(2)}$ and the optical intensity $I(2\omega)$ of this same field is proportional to the electric field squared, we get that the larger $\chi^{(2)}$ is the larger the $I(2\omega)$ of the frequency doubled beam will be. We are therefore interested in searching for systems where the hyperpolarizability is maximized. Throughout this work, we will be considering specifically second-harmonic generation in the off-resonant case $\omega = \omega' = \omega'' = 0$, where we can safely apply perturbation theory without worrying about resonant response.

The problem with attempting to maximize β from either (1.84) or any other expression for this quantity is that it is too complex of a process to do analytically. This makes it a good target for optimization schemes, in particular ones that do not depend on derivatives of the function to be optimized, in an attempt to find optimal solutions (as a maximum is not guaranteed with these schemes). We can therefore turn to a method of

this kind, using the potential energy of the system as the optimization variable which is to be iteratively altered until an optimal value of β is found.

The search of the maximum for the off-resonant hyperpolarizability for one-electron systems is the subject of research of several publications [10, 17, 21, 22] by Mark Kuzyk and others. In their work, the focus is on the search of a maximum for the *intrinsic* hyperpolarizability β_{int},

$$\beta_{int} = \frac{\beta}{\beta_{max}}, \tag{3.2}$$

a quantity used as a figure of merit that consists on the normalization of the calculated hyperpolarizability with respect to the maximal value a diagonal component of β can take when a 3-level ansatz is assumed for the system in the off-resonant case [7, 8, 11], given by

$$\beta_{max} = \sqrt[4]{3}\left(\frac{e\hbar}{\sqrt{m}}\right)\frac{N^{3/2}}{E_{10}^{7/2}}, \tag{3.3}$$

with N the number of electrons of the system under analysis and E_{10} its energy gap between the ground and first excited-states. This was always done for the case of 1-dimensional systems, as the authors found that for higher-dimensional cases the same or worse results are found.

The Nelder-Mead minimization method with potentials described by piecewise functions starting from some analytic expression (e.g. $v_0 = x^2$, $\tanh(x)$, etc) are used throughout these publications. In them, the conclusion was that, regardless of the initial function and the different conditions used for the potential, the maximal β seemed to always fall short of β_{max}, with β_{int} taking the apparent limit $|\beta_{int}| < 0.709$. Another important conclusion to take from this series of papers is that several different potentials seem to yield a value for β_{int} close to this apparent fundamental limit. This means that β appears to have more than one maximum, something that we will return to later on.

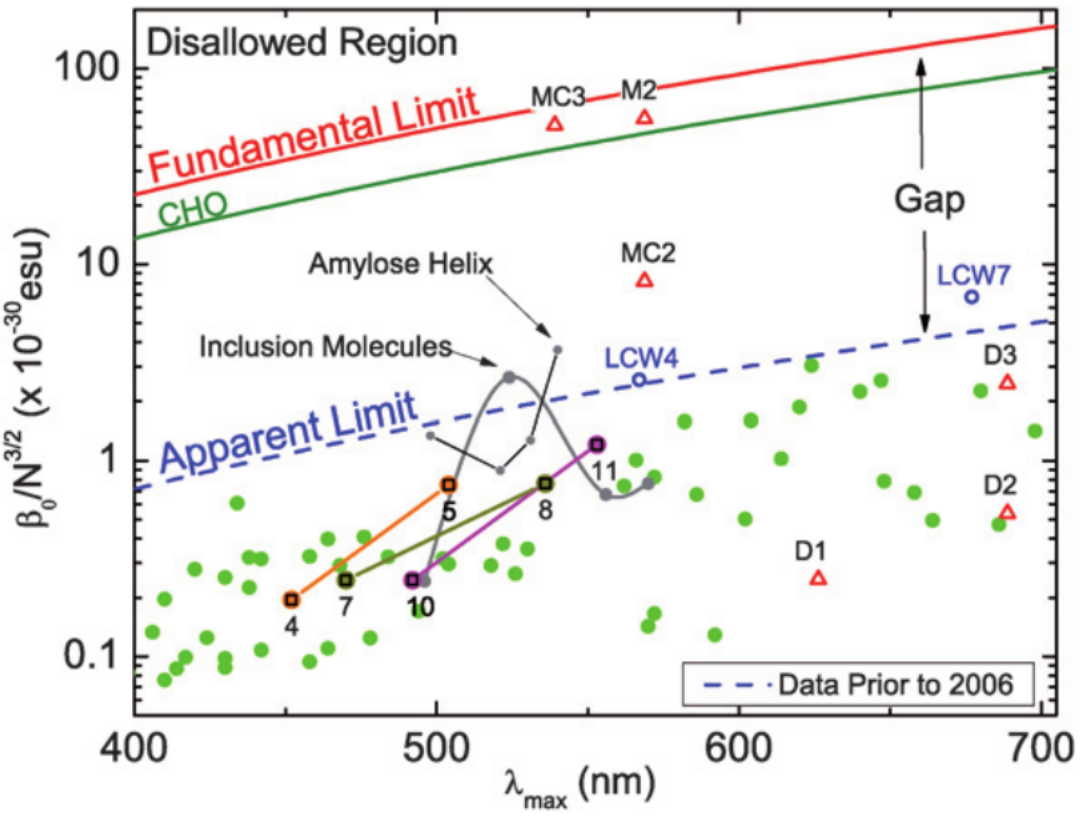

Figure 3.1: Plot of $\beta(\omega = 0)$ normalized to $N^{3/2}$ vs wavelength of the maximum absorbance of the first excited state within Kuzyk's 3-level approximation. The red line represents the theoretical limit within this framework, the green line corresponds to the case of the clipped harmonic oscillator, the dashed blue line is the apparent limit ($\beta_{int} = 0.709$ in the off-resonant case) and the green dots are experimental data.[9]

In the present work, the goal is to study what happens to the maximum β when interactions are switched on, i.e. what differs between a system with two non-interacting electrons and one with two interacting electrons. For a system where the two electrons are independent the value of beta will double when compared to the one electron case; the effect interactions have however is not obvious and thus demands a closer look. This is done strictly for the 1-dimensional case.

A study on this kind of systems has been done in [20], where the authors work within the same framework as the one mentioned above, optimizing β_{int} instead of β and assuming the 3-level ansatz. In it, a simple model is assumed for the interactions where they are composed of piecewise linear expressions of electrostatic and spin interaction terms, and it is concluded by the authors that the same universal properties previously observed for the one-electron systems are preserved, in particular that $|\beta_{int}| < 0.709$.

In this work, we aim to do a more general study of both the independent electrons

case and of what happens with interactions allowed. In order to do this, we use a genetic algorithm with the goal of maximizing the absolute value of β. This algorithm generates the potentials as Lagrange interpolations of a set of numbers chosen from a given range (the individuals); this allows for a wide range of potentials to be considered initially instead of a fixed function as the aforementioned work has done. Together with the fact that they are usually much faster at finding optimal solutions when compared to optimization methods like the Nelder-Mead simplex-based one, genetic algorithms are in theory great tools for this kind of problem, especially when dealing with such a complex function like β.

Another approach that differs from previously mentioned work is the framework from which calculations are done. Instead of using an approach based on finite differences in order to calculate β (Eq. (3) of [22]), we work in the TDDFT framework, where we do the calculation using the Sternheimer method and the $(2n + 1)$ theorem. The difference between these methods comes from the fact that in the case of finite differences we require the knowledge of the exact (or at least a very good approximation) wavefunction for every value of the electric field considered, whereas using (1.84) requires only the ground-state and first-order response wavefunctions (since we calculate the ground-state at zero field), as well as k_{xc} from (1.62) in the case of the interacting system. Using TDDFT also means that interactions between electrons can be dealt with without resorting to models like what was done in [20].

As working within TDDFT can lead to some time consuming calculations in the case of interacting electrons, it is interesting to compare the Nelder-Mead algorithm and our genetic algorithm on how time consuming they are. Let us suppose we are only interested in the most optimal value returned by the genetic algorithm for the sake of a direct comparison between the methods. Let us also suppose we have a population with size N, in which each individual has size S and which takes G generations to reach the optimum value. If each TDDFT calculation takes an amount of time T from start to finish, then the genetic algorithm takes a total amount of time $T_{GA} = N \times T \times G$. In the case of using the Nelder-Mead algorithm, building the potential from our size S individual as well and with the same amount of time per TDDFT calculation T, the time required to reach the optimum value is given by $T_{NM} = (S + 1) \times T \times I$, where I is the number of iterations it takes for the algorithm to converge and $(S + 1)$ is the size of the simplex. This means that as long as $N \times G$ is smaller than $(S + 1) \times I$ (which in general is the case), the genetic algorithm is faster, and is therefore a good approach to this optimization problem if it manages to reach optimal values similar to those obtained via the Nelder-Mead method.

Chapter 4

Results And Discussion

4.1 The Genetic Algorithm

The genetic algorithm used for this optimization procedure consists on two Python scripts, one for generating the individuals and building the file hierarchy needed for the DFT and TDDFT calculations and one for applying the GA operators and creating the next generation's population, and one Linux shell script that both runs the calculations and ensures the scripts are ran automatically in a correct order. The algorithm is summarized in Figure 4.1:

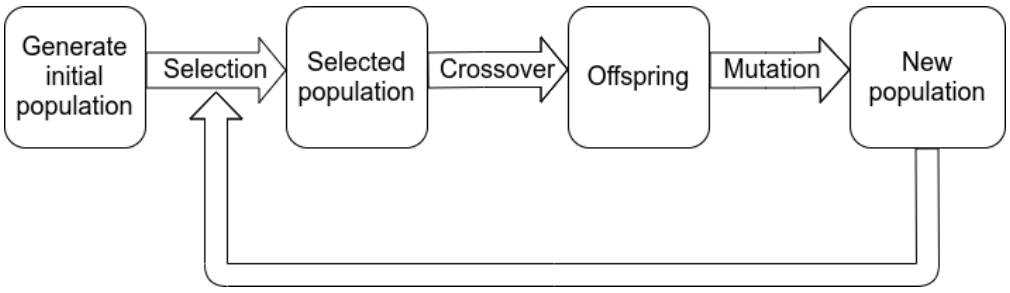

Figure 4.1: Flowchart with the summary of the genetic algorithm. The process is to be repeated until convergence.

The DFT and TDDFT calculations occur immediately after each of the population generation processes (the "Generate initial population" and "New population" boxes in Figure 4.1).

The individuals of the initial population are defined as follows. First, a "box", which due to the problem being one-dimensional is just a straight line, is generated, ranging from -10 to 10 a_0 (a_0 being the Bohr radius). The size of this "box" is the size of the system. Then, we define n points along this line using the n zeros of the Chebyshev polynomial of the first kind and degree n, $T_n(x)$. The degree n is the size of the individual. Finally, a potential value is attributed to each of this n points, with these values being

randomly generated from within a given range. It is the values of the potential in these fixed points that defines the individual.

Having a set of pairs of points in the "box" representing our system and corresponding potential values, we do a Langrange interpolation in order to have an analytic expression for the potential, which will allow us to do the necessary DFT and TDDFT calculations. Generating the points from the zeros of the aforementioned Chebyshev polynomial will be helpful for the calculations since this method has the desired feature of generating more points towards the ends of the mesh, thus making the polynomial less likely to blow up to extremely large values in those points and therefore making it more likely to be well behaved. This analytic expression for the potential will be the individual from the physical point-of-view.

This algorithm relies only on crossover and mutations as its GA operators. The crossover operator is defined in the following way:

1. two individuals are selected for crossover;

2. a) 50% of the time a two-point crossover (where two gene positions in the two individuals selected for crossover are randomly chosen, and the genes in those positions are interchanged) is executed;
   b) the other 50% of the time there is a 50% chance for each gene position that a different crossover operation occurs. For this, there is a 50% chance for each gene position selected that the corresponding gene in each individual is changed into the sum of the genes in that position for both individuals and a 50% chance that it is changed to their average value.

The goal for this crossover operator is for a larger part of the search space to be run through via crossover than the possible combinations of genes from the initial population.

As for the mutation operator, a gaussian mutation centered on zero and with a σ of 40% of the maximum potential value allowed is used. This operator will have a 50% chance to be applied to each individual. When an individual is selected for mutation, each of its genes then has a 10% chance to be mutated. This means that for an individual with 29 genes, on average 2.9 of its genes will be mutated. It is worth noting that the mutation being based on a gaussian distribution means that it has the possibility of generating genes outside of the range defined for the individuals of the initial population, just like the crossover operator, giving it the possibility to broaden the search space for the genetic algorithm.

The selection process used for this algorithm is an elitist one, where the best 50% individuals, i.e. the ones with largest β, are selected for breeding. Before this process occurs there is however a previous screening done in order to exclude individuals with unwanted characteristics regarding their ground-states, like them being degenerate. This is done by setting their β to 0 in case the HOMO-LUMO gap is less than a certain amount (in our case defined to be 0.5 eV). As the quantity to be optimized is the β's *absolute value*, these individuals are immediately excluded in the selection process.

4.2 TDDFT Calculations

All calculations were done using the OCTOPUS code. A one-dimensional grid with radius 10.0 a_0 and a spacing of 0.01 a_0 was used for all individuals. This means that the systems considered have a fixed size of 20 a_0. In the interacting cases, the LDA exchange in one-dimension and the Casula, Sorella, and Senatore functional for the one-dimensional correlation [2] were used, as well as the average-density self-interaction correction [13]. In the ground-state calculations, the first excited-state is also calculated in order to calculate the HOMO-LUMO gap, not only for the exclusion of degenerate ground-states but also for an eventual calculation of the β_{int}. All quantities presented are in atomic units.

4.3 Results

Before going through what happens when going from two independent electrons to two interacting ones, we first run the genetic algorithm for the case of one electron only. This serves not only to see if the algorithm is working properly, but also to tune the necessary hyperparameters like the population size, the length of the individuals, the range of initial potential values allowed, etc. The optimal range found from this tuning process was (-1,1) Hartree, with the results improving with increasing individual length. The largest length admitted by the code while keeping the interpolation precise, 29, was thus chosen. This was hinted already by Kuzyz et. al., noting in their work that a substantial degree in complexity was needed for the potentials to be the most optimal.

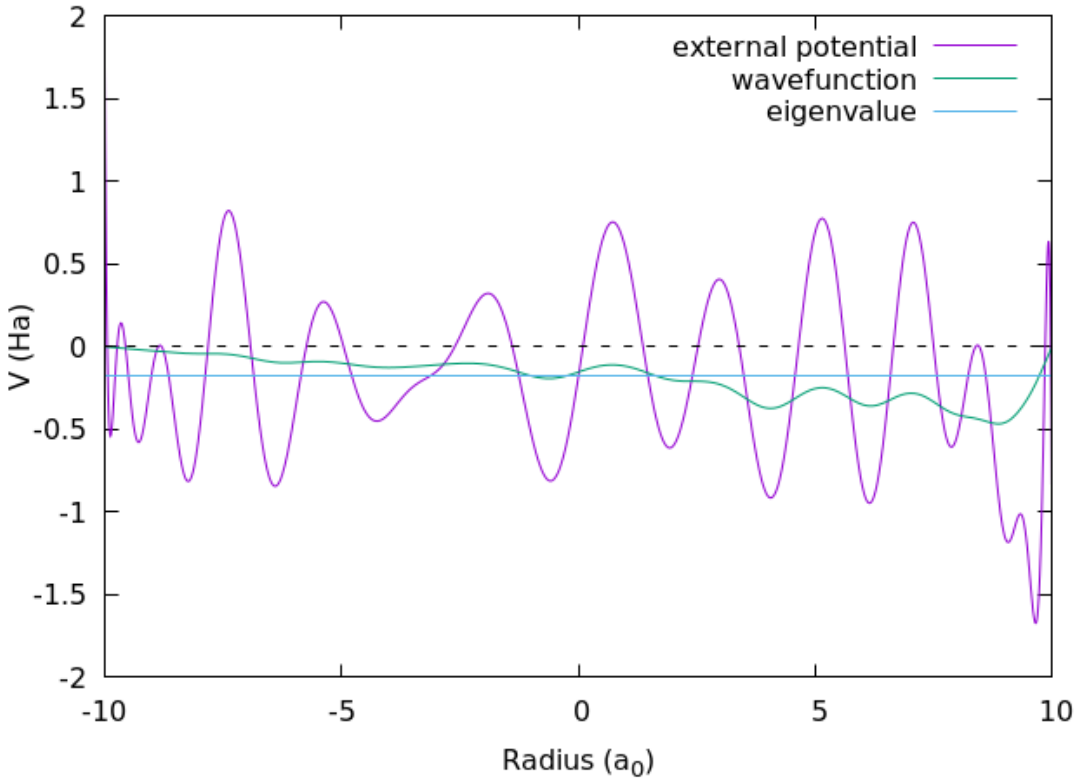

Figure 4.2: Potential energy vs position on the grid for the best individual after convergence in the case of individual length 29 of a one-electron system. The electron's eigenvalue is also plotted, with its value being -0.174592 Ha. The absolute value of beta for this case was $|\beta| = 1.35 \times 10^6$ a.u.

From Figure 4.2 we can see that the wavefunction is very delocalized, growing in absolute value in regions where the potential is decreasing and shrinking when it is increasing. It is also worth to note that β_{int} for the most optimal individual was found to be larger than the reported apparent maximum value of $|\beta_{int}| = 0.709$. This goes against what was found in the papers mentioned in Chapter 3.

Fixing the initial potential values range at (-1,1) and the length of the individuals at 29, we now turn to see what happens when going from a system with 2 independent electrons to a system with 2 interacting ones.

In the case of two non-interacting electrons, we find (as expected) that the value for $|\beta|$ approximately doubles, with nothing noteworthy changing regarding the wavefunctions (which coincide for spin-up and spin-down, as expected) and potential.

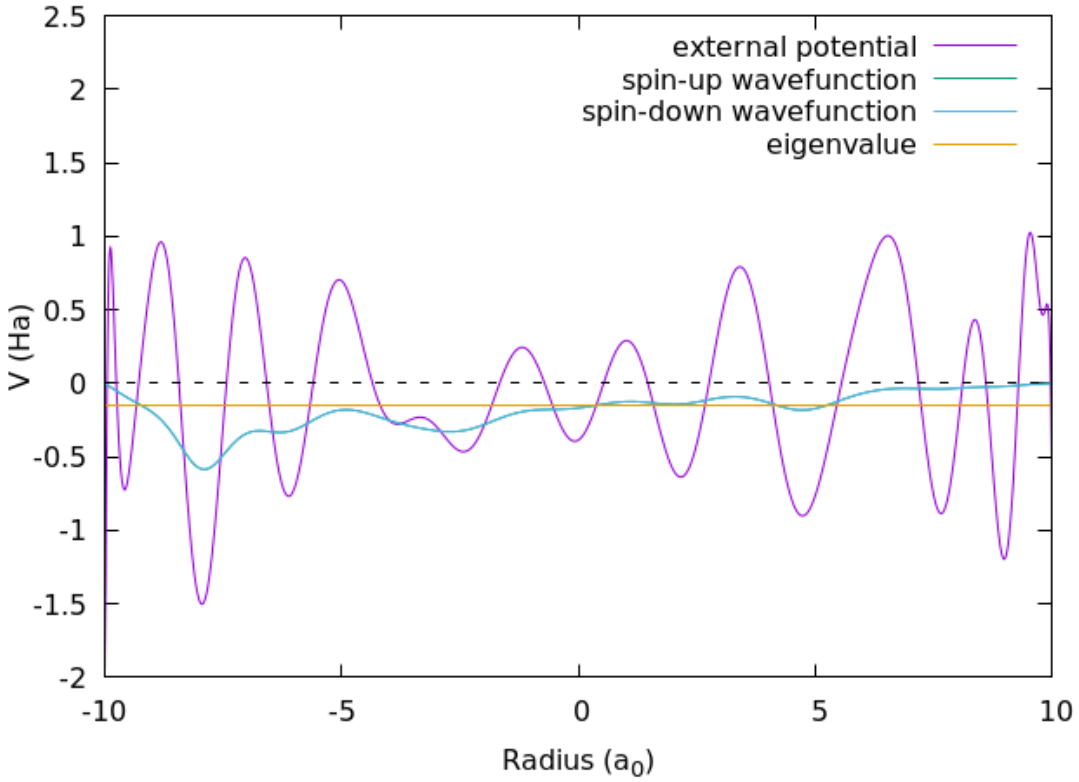

Figure 4.3: Potential energy vs position on the grid for the best individual after convergence in the case of individual length 29 of a two independent-electron system. The eigenvalue for both electrons is -0.146545 Ha. The absolute value of beta for this case was $|\beta| = 2.27 \times 10^6$ a.u.

When interaction is turned on, however, a massive (10 orders of magnitude) increase of β occurs. As can be seen in Figure 4.4, the wavefunction is much more localized (the spin-up and spin-down wavefunctions still coincide, as expected), with the region of the potential where its majority is located being very wide in comparison to the previous cases. The potential is also much less oscillating in general. There is therefore a noticeable change in behaviour in the interacting case associated with the huge increase in β, showing that it is in this framework that remarkably high hyperpolarizabilities can be obtained.

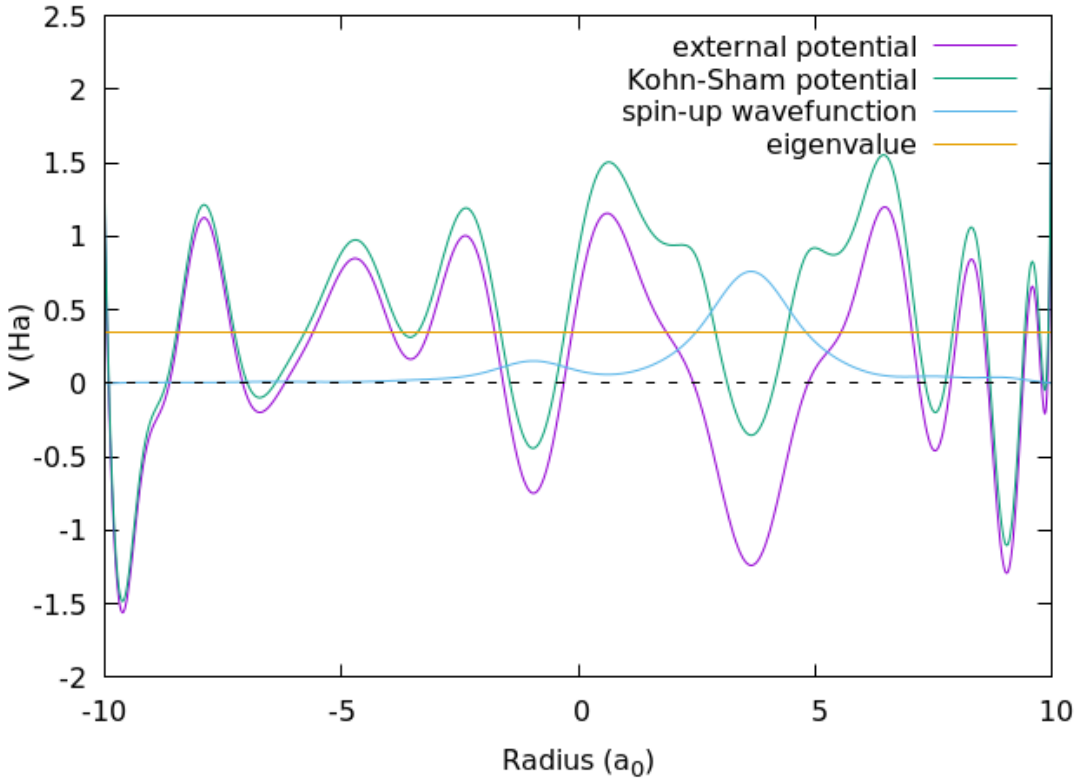

Figure 4.4: Potential energy vs position on the grid for the best individual after convergence in the case of individual length 29 of a two interacting-electron system. The eigenvalue for both electrons is 0.348287 Ha. The absolute value of beta for this case was $|\beta| = 4.78 \times 10^{16}$ a.u.

As in the one electron case, we find that β_{int} is higher than what was obtained by Kuzyk et. al.; however, in this case it not only surpasses the apparent limit of the 3-level model but is also *greater* than the maximum value of $\beta_{int} = 1$ predicted in it by 11 orders of magnitude. The interacting optimal individual therefore appears to contradict this model. We also note that the eigenvalue for the electrons is now positive. This is a general trend for the best individuals of the interacting case (see Appendix B).

The sharp increase in the optimal values of β is not, however, without problems for the algorithm. By turning the interactions on in our systems, a significant number of individuals whose associated calculations were previously well behaved begin to not converge. The reason for these anomalies can be seen by comparing the plots for a given individual's potentials and wavefunctions in the non-interacting and interacting frameworks in the case of an individual whose calculation of β does not converge when interactions are turned on. It is worth noting that the external potential is the same in both cases, but in the non-interacting case it also coincides with the Kohn-Sham potential, i.e. $v_{ext} = v_s$.

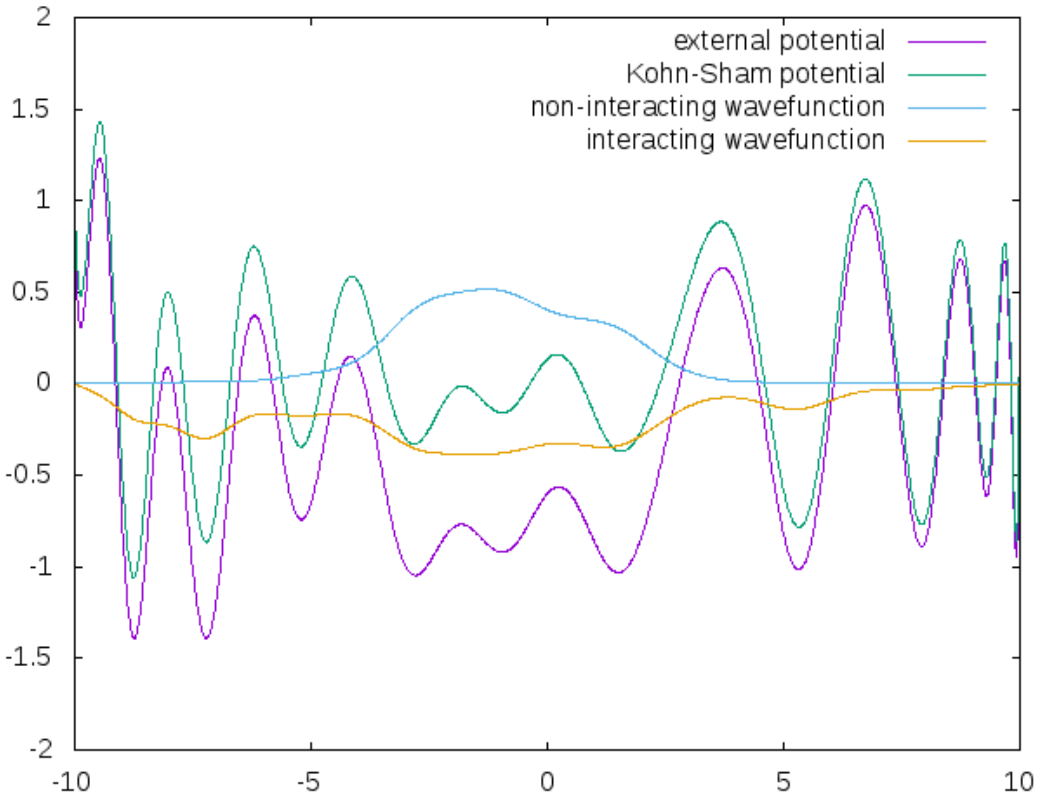

Figure 4.5: Potential energy vs position on the grid for an individual of length 29 with non-converged β in the two interacting-electron case and converged in the non-interacting one, with absolute value $|\beta| = 1.74 \times 10^2$ a.u.

Figure 4.5 shows that for this case the interaction makes the potential rise everywhere, with this increase being more steep in the region where the wavefunction has higher values, as expected from the Hartree term. The wavefunction itself is also changed, being less localized than in the non-interacting case. It is also worth noting that the potential does not change significantly in shape in the region where the wavefunction is higher valued between both cases.

Figure 4.6, on the other hand, portrays the case of the individual that optimizes $|\beta|$ for two interacting-electrons, with the difference from Figure 4.4 being that we also plot the non-interacting wavefunction. Contrary to the individual depicted in Figure 4.5, this one also converges in the non-interacting case. Despite the fact that some characteristics are the same as in the previous analysis (vertical shift in the potential when going from the non-interacting system to the interacting one and less localized wavefunction), we now get a major increase in $|\beta|$. This could be due to the change in the shape of the potential that occurs when interactions are turned on.

To further emphasize how much the shape of the potential has an effect on the hyperpolarizability, let us compare Figure 4.6 with a very similar potential arising from this optimization procedure, depicted in Figure 4.7. Despite the similarities, we see an

increase in $|\beta|$ when going from Figure 4.7 to Figure 4.6 of 2 orders of magnitude. These examples thus serve to show that β is a highly non-linear quantity, which can massively change in value even when subjected to very similar potentials.

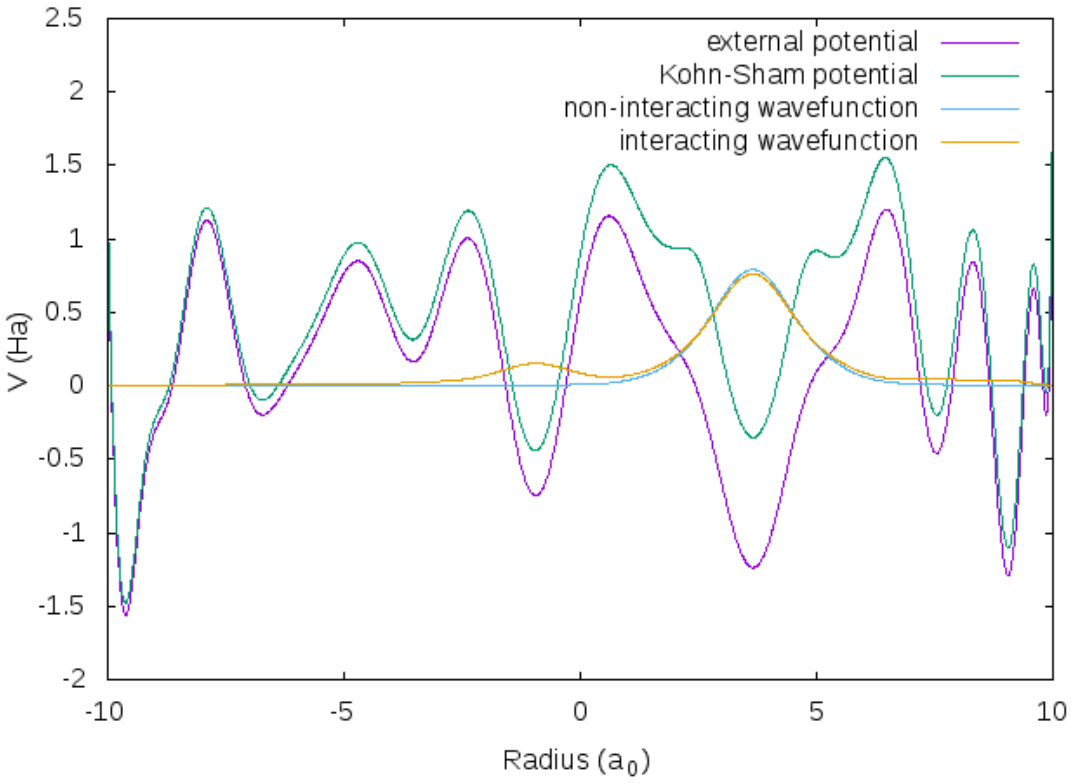

Figure 4.6: Potential energy vs position on the grid for the same individual as in Figure 4.4, now in both the interacting and non-interacting cases. For the latter we get $|\beta| = 8.69 \times 10^{-3}$ a.u.

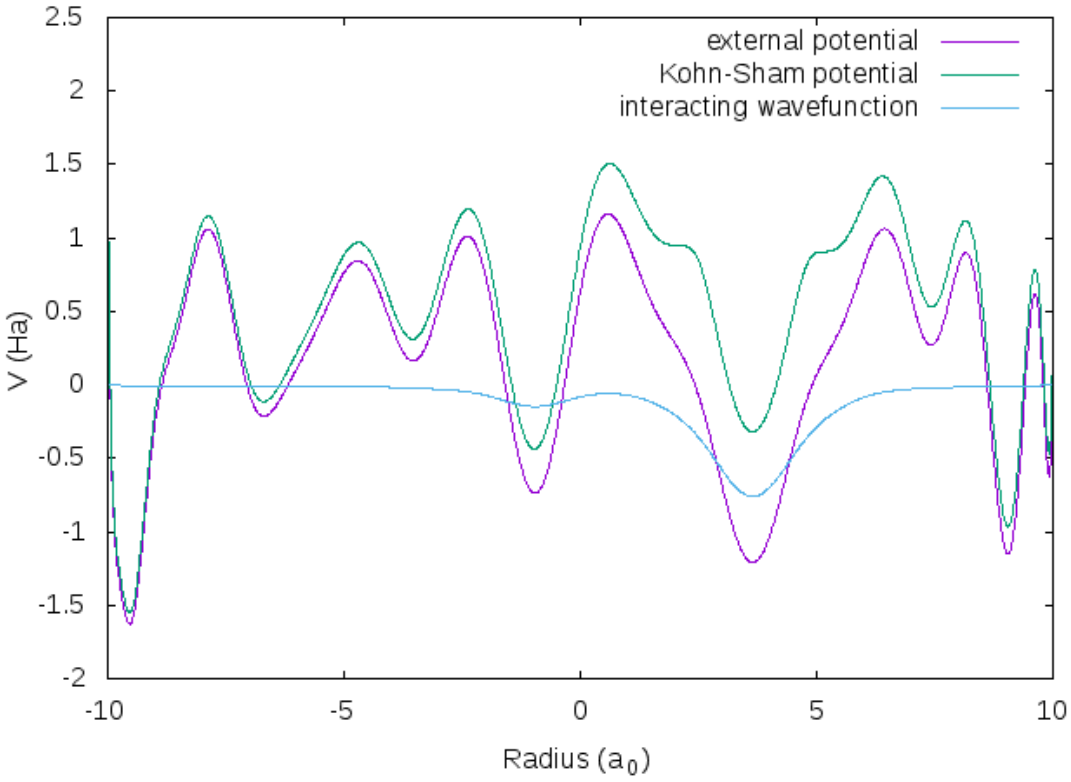

Figure 4.7: Potential energy vs position on the grid for an individual similar in shape to the most optimal one from the two interacting-electron case, with $|\beta| = 3.64 \times 10^{14}$ a.u.

Chapter 5

Conclusions And Future Work

In summary, we are able to both show that the genetic algorithm implemented works well as a tool for the optimization of the hyperpolarizabilty, and that interaction in a two-electron system leads to a sharp (11 orders of magnitude in the optimization process shown previously) increase in the value of $|\beta|$ of the optimized individuals when compared to the non-interacting case (see Appendix B). It is also found that despite there not being a significant change in the behavior of the potential and the wavefunctions when going from one to two non-interacting electron systems, when interaction is turned on there is a clear increase in the localization of the wavefunction, with the potential increasing in width in this same region.

Another interesting find was that the values of β_{int} for the one-electron and two interacting-electron cases are larger than the ones obtained by Kuzyk et. al., with the value found when interaction is present even surpassing the maximum value of $\beta_{int} = 1$ predicted by the 3-level model, and thus appearing to contradict it. Further work on this point is thus needed, especially a more direct comparison by using the optimized individuals and calculate their hyperpolarizability the same way as in Kuzyk et. al.'s work.

Additionally, by comparing the potentials and wavefunctions for a given individual in the two-electron non-interacting and interacting cases we see that slight changes in the shape of the potential and/or on its value can lead to massive changes in the hyperpolarizability. This is a testament to how highly non-linear β is and how details are crucial when dealing with the calculation and optimization of this quantity.

Finally, the transition of the eigenvalues from negative to positive values when going from the non-interacting to the interacting case is also worth highlighting. Literature suggests [19] there is a relationship between the increase in hyperpolarizability and the existence of bound-states in the continuum. This cannot however be concluded to happen for our case, since the asymptotic value of the potential is not conditioned a priori. Furthermore, by imposing nullifying boundary conditions we make it difficult to distinguish between continuum states and box states. Since the potential is given by Lagrange interpolation, it is tricky to impose conditions that guarantee the desired behavior to study this phenomena in the optimization procedure. An attempt to reduce

this problem was made by demanding the total energy of the individuals to be negative, thus making the minimum value of the potential negative as well. This is, however, an insufficient and artificial condition to impose and it has to be improved upon. This is surely a path we ought to explore in the future in our search for a reason behind the sharp increase in β observed.

Appendix A

Density Functional Theory

A.1 The Hohenberg-Kohn Theorem

As stated previously (see chapter 1.1), Density Functional Theory works as an exact reformulation of the time-independent many-body problem for the ground-state of the system. The motivation for this is the same as in the time-dependent case: the wavefunction Ψ scales exponentially with the number of electrons, making its usage non-viable in most cases. The fundamental theorems of DFT solve this issue by showing that the charge-density $n(\boldsymbol{r})$ of the ground-state (the time-independent version of (1.15))is enough to calculate any ground-state and excited-state expectation-value of the system. This is done via the Hohenberg-Kohn theorem [6], which we prove next for the spin-unpolarized case (see [14] for example for the spin-polarized case) in the case the ground-state is non-degenerate (the extension to degenerate ground-states is straightforward and can be seen in [3]).

From the solution of the time-independent Schrödinger equation we can establish a map from the external potential $v_{ext}(\boldsymbol{r})$ to the ground-state wavefunction Ψ and consequently to $n(\boldsymbol{r})$:

$$v_{ext}(\boldsymbol{r}) \rightarrow \Psi(\boldsymbol{r}) \rightarrow n(\boldsymbol{r}). \tag{A.1}$$

By showing that this map is one-to-one, and therefore fully invertible, we obtain the map

$$v_{ext}(\boldsymbol{r}) \leftrightarrow n(\boldsymbol{r}), \tag{A.2}$$

thus showing that $v_{ext}(\boldsymbol{r})$ is a unique functional of $n(\boldsymbol{r})$ up to an additive constant.

In order to demonstrate the first arrow of (A.1), we begin by assuming that we have two external potentials $\hat{V}_{ext}$ and $\hat{V}'_{ext}$ such that $\hat{V}_{ext} \neq \hat{V}'_{ext} + c$, with c a constant. The respective Hamiltonians for the unprimed and primed systems are

$$\hat{H} = \hat{F} + \hat{V}_{ext} \tag{A.3}$$
$$\hat{H}' = \hat{F} + \hat{V}'_{ext} \tag{A.4}$$

respectively, where $\hat{F}$ represents all other operators from the Hamiltonian. This operator is the same for both systems since it is independent of the external potential and depends only on the number of electrons. If we assume both $\hat{V}_{ext}$ and $\hat{V}'_{ext}$ lead to the same ground-state wavefunction Ψ_0, then by applying $\hat{H}$ and $\hat{H}'$ to it and subtracting them we obtain

$$(\hat{F} + \hat{V}_{ext}) |\Psi_0\rangle - (\hat{F} + \hat{V}'_{ext}) |\Psi_0\rangle = E |\Psi_0\rangle - E' |\Psi_0\rangle , \tag{A.5}$$

and therefore,

$$(\hat{V}_{ext} - \hat{V}'_{ext}) |\Psi_0\rangle = (E - E') |\Psi_0\rangle . \tag{A.6}$$

As both E and E' are constants, this contradicts our initial statement about the potentials. This proves that up to a constant the external potential determines the ground-state wavefunction.

To prove the second arrow in (A.1), we now assume we have two different ground-state wavefunctions Ψ_0 and Ψ'_0 that lead to the same charge density $n(\boldsymbol{r})$. Using the Rayleigh-Ritz variational principle we get

$$E_0 = \langle \Psi_0 | \hat{H} | \Psi_0 \rangle < \left\langle \Psi'_0 \right| \hat{H} \left| \Psi'_0 \right\rangle . \tag{A.7}$$

We also have

$$\left\langle \Psi'_0 \right| \hat{H} \left| \Psi'_0 \right\rangle = \left\langle \Psi'_0 \right| \hat{H}' + \hat{V}_{ext} - \hat{V}'_{ext} \left| \Psi'_0 \right\rangle = E'_0 + \left\langle \Psi'_0 \right| \hat{V}_{ext} - \hat{V}'_{ext} \left| \Psi'_0 \right\rangle , \tag{A.8}$$

and therefore

$$E_0 < E'_0 + \left\langle \Psi'_0 \right| \hat{V}_{ext} - \hat{V}'_{ext} \left| \Psi'_0 \right\rangle . \tag{A.9}$$

By a completely analogous way we get

$$E'_0 < E_0 + \langle \Psi_0 | \hat{V}'_{ext} - \hat{V}_{ext} | \Psi_0 \rangle . \tag{A.10}$$

Since we assumed both Ψ_0 and Ψ'_0 lead to the same density, we have

$$\begin{aligned}
&\left\langle \Psi_0' \right| \hat{V}_{ext} - \hat{V}_{ext}' \left| \Psi_0' \right\rangle = \int n'(\boldsymbol{r})(v_{ext}(\boldsymbol{r}) - v_{ext}'(\boldsymbol{r}))d^3r \\
&= \int n(\boldsymbol{r})(v_{ext}(\boldsymbol{r}) - v_{ext}'(\boldsymbol{r}))d^3r = -\int n'(\boldsymbol{r})(v_{ext}'(\boldsymbol{r}) - v_{ext}(\boldsymbol{r}))d^3r \\
&= \left\langle \Psi_0 \right| \hat{V}_{ext}' - \hat{V}_{ext} \left| \Psi_0 \right\rangle . \qquad \text{(A.11)}
\end{aligned}$$

We can therefore sum (A.9) and (A.10) to obtain

$$E_0 + E_0' < E_0 + E_0'. \qquad \text{(A.12)}$$

This is again a contradiction, which proves that different ground-state wavefunctions necessarily lead to different charge densities. We note however that this proof (particularly the usage of the Rayleigh-Ritz variational principle) holds in this exact form only because we are considering non-degenerate ground-states, and that the general proof is not exactly the same.

We have therefore proven both right-pointing arrows in (A.1) are one-to-one in nature, i.e. both the map from external potential to the ground-state wavefunction and from that to the charge density are injective, and therefore the composite map from the potential to the density is injective and thus invertible. This is represented by (A.2).

The Hohenberg-Kohn theorem can therefore be stated as follows: for a given interacting many-body system, the external potential and the ground state density are related by a one-to-one correspondence. This means that not only the charge density is a functional of $v_{ext}(\boldsymbol{r})$, which comes from the solution of the Schrödinger equation, but the inverse is also true, and we can write the external potential as $v_{ext}[n_0](\boldsymbol{r})$.

Since as stated before all other operators of the Hamiltonian are fixed, we immediately conclude that $\hat{H}$ itself is a functional of the density. This leads us to a pivotal consequence of the theorem: since we can write $\hat{H}$ as $\hat{H}[n_0]$, from the Schrödinger equation we get that *every* eigenstate of the system (not only the ground-state) is a functional of the density as well. We can therefore conclude that n_0 is in principle sufficient not only to calculate every ground-state observable of a many-body static system, but every *excited-state* observable as well, although this case is not very useful in practice since we do not know to obtain most of them, and therefore have to rely on other frameworks (like TDDFT) for their calculation.

The original paper by Hohenberg and Kohn also proves an important consequence of the aforementioned theorem. If we take the Hamiltonian from (A.3) with a given external potential $v_0(\boldsymbol{r})$, a unique ground-state wavefunction $\Psi_0[n_0]$ and density $n_0(\boldsymbol{r})$, we easily see using the Rayleigh-Ritz variational principle that

$$\left\langle \Psi_0[n_0] \right| \hat{H}[n_0] \left| \Psi_0[n_0] \right\rangle = E[n_0] < E[n'] = \left\langle \Psi_0'[n'] \right| \hat{H}[n_0] \left| \Psi_0'[n'] \right\rangle . \qquad \text{(A.13)}$$

This means that the ground-state density minimizes the energy, yielding the ground-state energy E_0. As a consequence, we have that n_0 can be found via minimization of the

energy functional with the constraint that particle number is to be conserved. Writing $E[n]$ as

$$E[n] = F[n] + \int d^3r n(\boldsymbol{r}) v_0(\boldsymbol{r}), \tag{A.14}$$

we obtain the following Euler-Lagrange equation

$$\frac{\delta}{\delta n(\boldsymbol{r})}\left[F[n] + \int d^3r' n(\boldsymbol{r}') v_0(\boldsymbol{r}') - \mu \int d^3r' n(\boldsymbol{r}')\right] = 0, \tag{A.15}$$

where μ is the Lagrange multiplier associated with the particle number constraint. This finally leads us to

$$\frac{\delta F[n]}{\delta n(\boldsymbol{r})} + v_0(\boldsymbol{r}) = \mu, \tag{A.16}$$

and the density which correctly solves this equation is then the ground-state density.

A.2 The Kohn-Sham Scheme

With (A.16) we see that the problem of finding the ground-state density is reduced to finding an expression for $F[n]$. This is however a very difficult task to do for our interacting many-body system due to the inherent difficulties presented arising from the electron-electron interactions, making this method unappealing for finding n_0. The ingenious step taken by Kohn and Sham was to realize that this problem could be solved by rewriting the energy functional as follows:

$$\begin{aligned} E[n] &= F[n] + v_{ext}[n] = T[n] + V_{ee}[n] + v_{ext}[n] \\ &= T_s[n] + \frac{1}{2}\int d^3r \int d^3r' \frac{n(\boldsymbol{r}) n(\boldsymbol{r}')}{|\boldsymbol{r} - \boldsymbol{r}'|} + \int d^3r n(\boldsymbol{r}) v_{ext}(\boldsymbol{r}) + E_{xc}[n]. \end{aligned} \tag{A.17}$$

In this last equality, the second and third terms correspond to the classical electrostatic electron-electron interaction and the external potential energies respectively; the first term corresponds to the kinetic energy of a system with the density $n(\boldsymbol{r})$ if it were non-interacting, and the last term is the remaining part of the energy, the exchange-correlation energy. By rewriting the energy in this way, we are effectively considering the system in a fictional frame, with the same density of the original interacting one but non-interacting in nature, subject to an external potential $v_s[n]$ only (the often-called Kohn-Sham potential), comprised of the functional derivatives of the last three terms of (A.17):

$$v_s[n](\boldsymbol{r}) = \int d^3r' \frac{n(\boldsymbol{r}')}{|\boldsymbol{r} - \boldsymbol{r}'|} + v_{ext}(\boldsymbol{r}') + v_{xc}[n](\boldsymbol{r}), \tag{A.18}$$

with

$$v_{xc}[n](\boldsymbol{r}) = \frac{\delta E_{xc}[n]}{\delta n(\boldsymbol{r})}. \tag{A.19}$$

With this now non-interacting system we can easily build the ground-state wavefunction, as it reduces to a Slater determinant (via the same arguments used for Hartree-Fock, see chapter 1) built like in (1.8), but with the orbitals now satisfying the one-electron Schrödinger equation

$$\left(-\frac{\nabla}{2} + v_s[n](\boldsymbol{r}) \right) \varphi_i(\boldsymbol{r}) = \epsilon_i \varphi_i(\boldsymbol{r}), \tag{A.20}$$

and with the ground-state density calculated from the occupied orbitals via

$$n_0(\boldsymbol{r}) = \sum_i |\varphi_i(\boldsymbol{r})|^2. \tag{A.21}$$

Equations (A.19) to (A.21) are the Kohn-Sham equations, and they constitute a much simpler but equivalent method to calculate n_0 than through (A.16).

A.3 The Local Density Approximation

The contents of the previous chapters show we can in principle deal with many-body interacting systems by working in a non-interactive fictitious one with the same density; this is however not without a cost. Although when working in the Kohn-Sham scheme we can calculate $T_s[n]$ exactly, $E_{xc}[n]$ has to be approximated.

The simplest approximation one can make in order to calculate $E_{xc}[n]$ is the Local Density Approximation (LDA) and it is based on the energy of the uniform electron gas. Within this approximation, we get that for a gas of density $n(\boldsymbol{r})$ any energy component $G[n]$ is given by

$$G^{LDA}[n] = \int d^3r n(\boldsymbol{r}) g^{LDA}(n(\boldsymbol{r})), \tag{A.22}$$

with $g^{LDA}(n(\boldsymbol{r}))$ the corresponding energy component per particle.

This leads us to an exchange energy-density e_x^{LDA} given by [4]

$$e_x^{LDA} = -\frac{3}{4\pi}\frac{(9\pi/4)^{1/3}}{r_s}, \tag{A.23}$$

with r_s the Seitz radius, defined by

$$r_s = \left(\frac{3}{4\pi n}\right)^{1/3}. \tag{A.24}$$

This corresponds to the radius of a sphere containing on average one electron.

As for the correlation energy, its expression is only known for two limiting cases. The first, known as the high-density or weak-coupling limit (where $r_s \to 0$), leads us to

$$e_c^{LDA} = c_0 \ln(r_s) - c_1 + c_2 r_s \ln(r_s) - c_3 r_s + ..., \tag{A.25}$$

with $c_i, i = 0, 1, ...$ constants. The second case is the low-density or strong-coupling limit (where $r_s \to \infty$), which results in

$$e_c^{LDA} = -\frac{d_0}{r_s} + \frac{d_1}{r_s^{3/2}} + ..., \tag{A.26}$$

with $d_i, i = 0, 1, ...$ constants.

One can write the correlation energy in such a way that comprises both limits:

$$e_c^{LDA} = -2c_0(1 + \alpha_1 r_s) \ln\left(1 + \frac{1}{2c_0(\beta_1 r_s^{1/2} + \beta_2 r_s + \beta_3 r_s^{3/2} + \beta_4 r_s^2)}\right). \tag{A.27}$$

Here, we have

$$\beta_1 = \frac{1}{2c_0} e^{-c_1/2c_0} \tag{A.28}$$

$$\beta_2 = 2c_0\beta_1^2, \tag{A.29}$$

with the other coefficients constant found by fitting to accurate Quantum Monte Carlo correlation energies for $r_s = 2, 5, 10, 20, 50$ and 100.[4]

Appendix B

Hall Of Fame From The Genetic Algorithm's Optimization

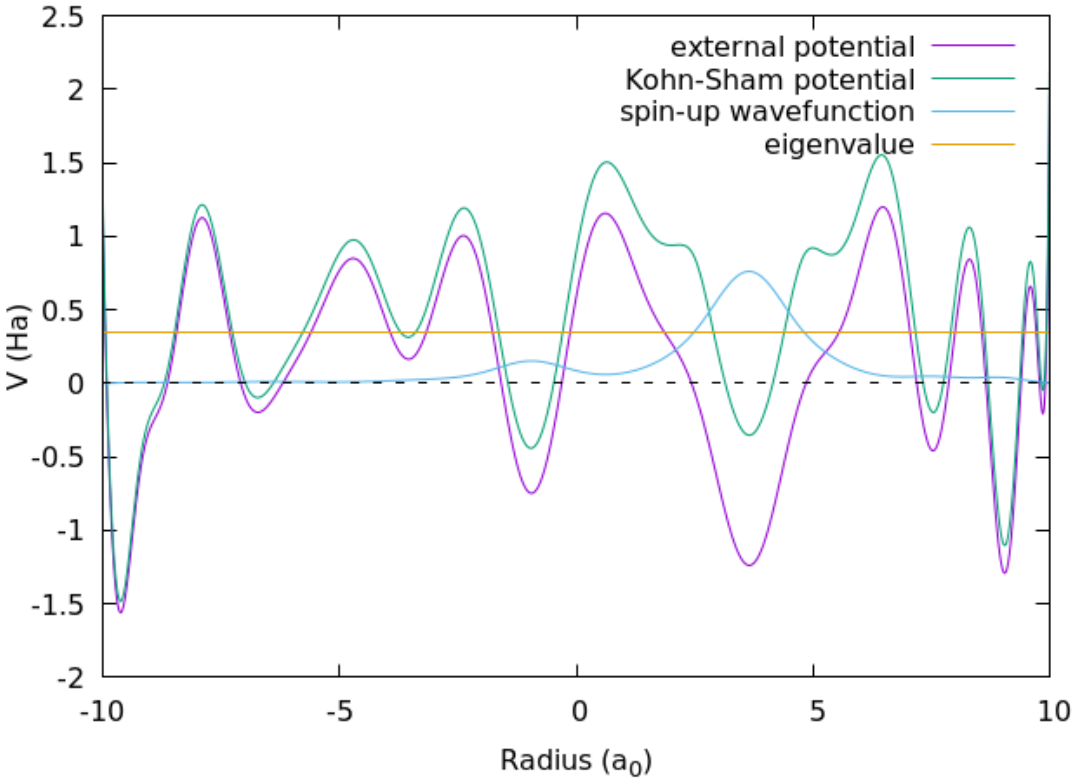

Figure B.1: Potential energy vs position on the grid for the best individual after convergence in the case of individual length 29 of a two interacting-electron system. The eigenvalue for both electrons is 0.348287 Ha. The absolute value of beta for this case was $|\beta| = 4.78 \times 10^{16}$ a.u.

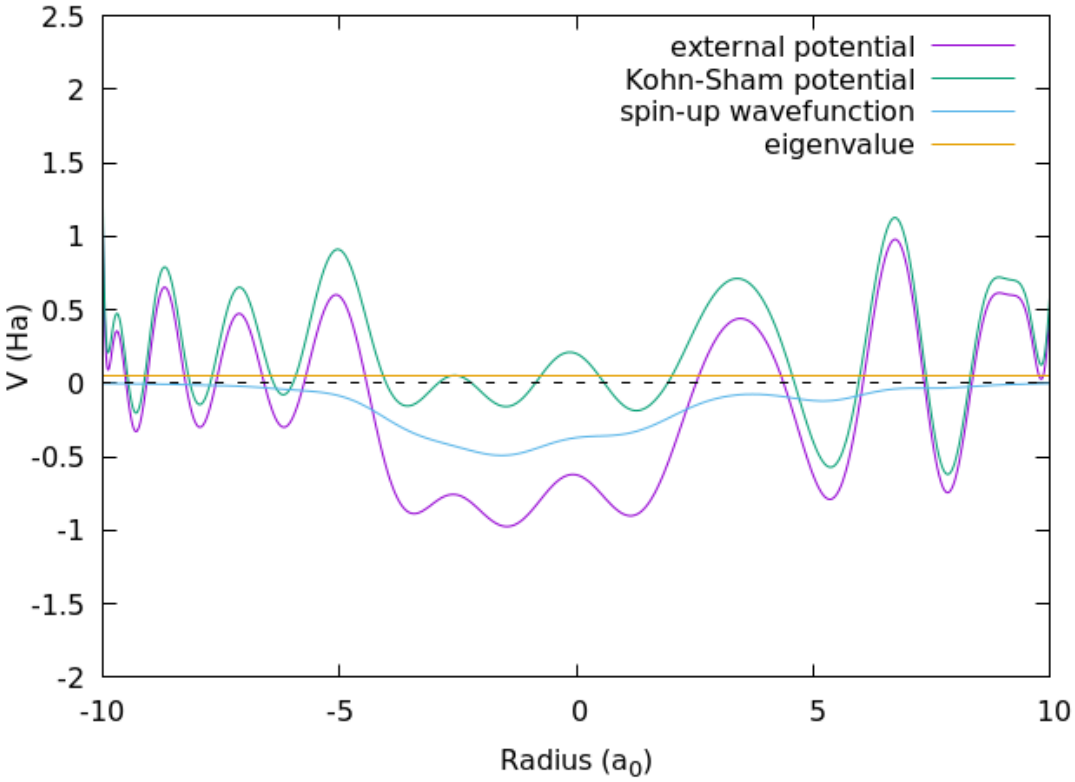

Figure B.2: Potential energy vs position on the grid for the second-best individual after convergence in the case of individual length 29 of a two interacting-electron system. The eigenvalue for both electrons is 0.049821 Ha. The absolute value of beta for this case was $|\beta| = 2.91 \times 10^{15}$ a.u.

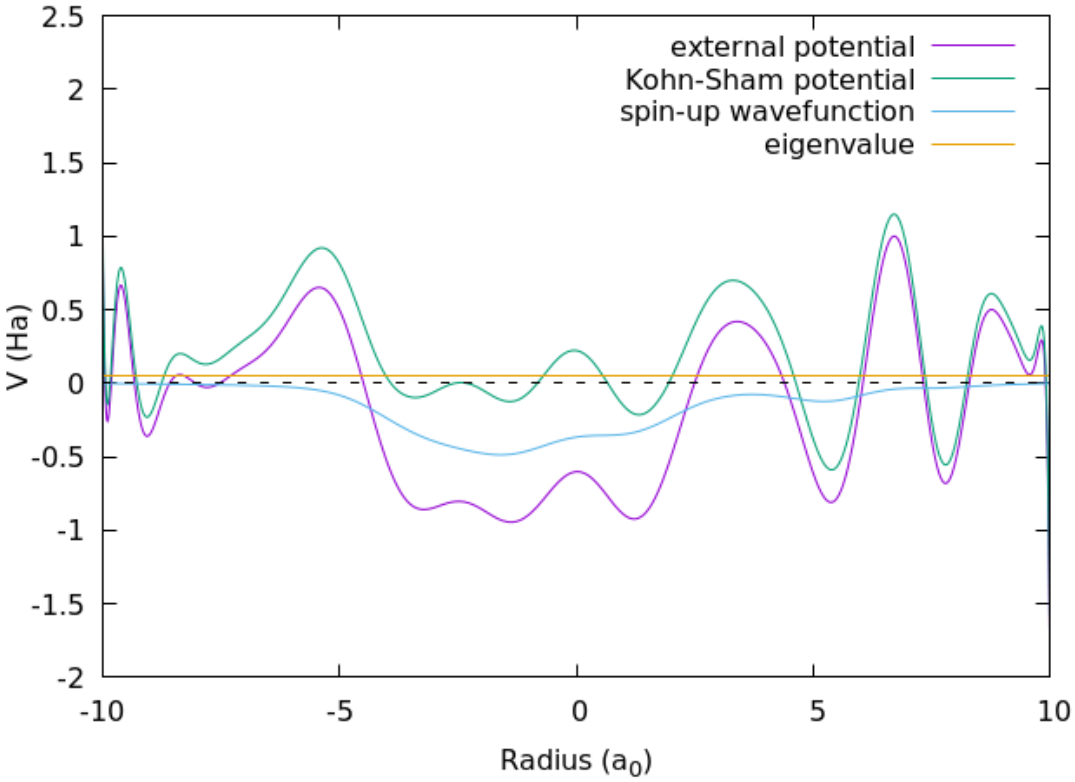

Figure B.3: Potential energy vs position on the grid for the third-best individual after convergence in the case of individual length 29 of a two interacting-electron system. The eigenvalue for both electrons is 0.052968 Ha. The absolute value of beta for this case was $|\beta| = 2.42 \times 10^{15}$ a.u.

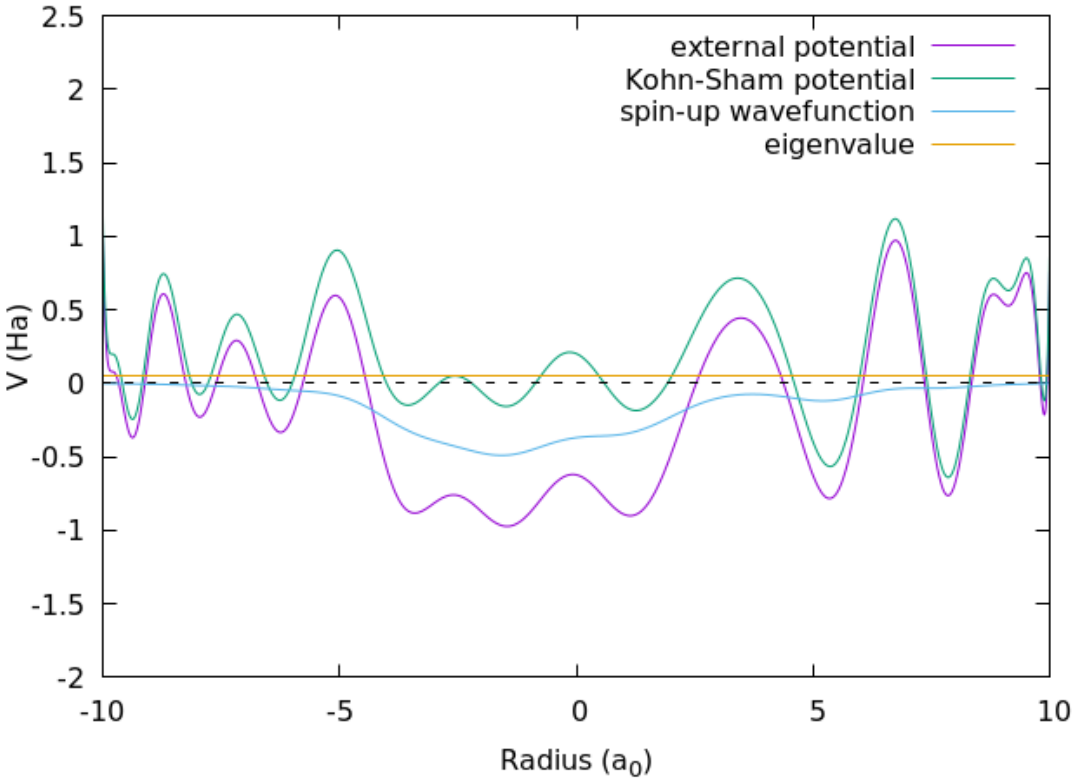

Figure B.4: Potential energy vs position on the grid for the fourth-best individual after convergence in the case of individual length 29 of a two interacting-electron system. The eigenvalue for both electrons is 0.049651 Ha. The absolute value of beta for this case was $|\beta| = 1.97 \times 10^{15}$ a.u.

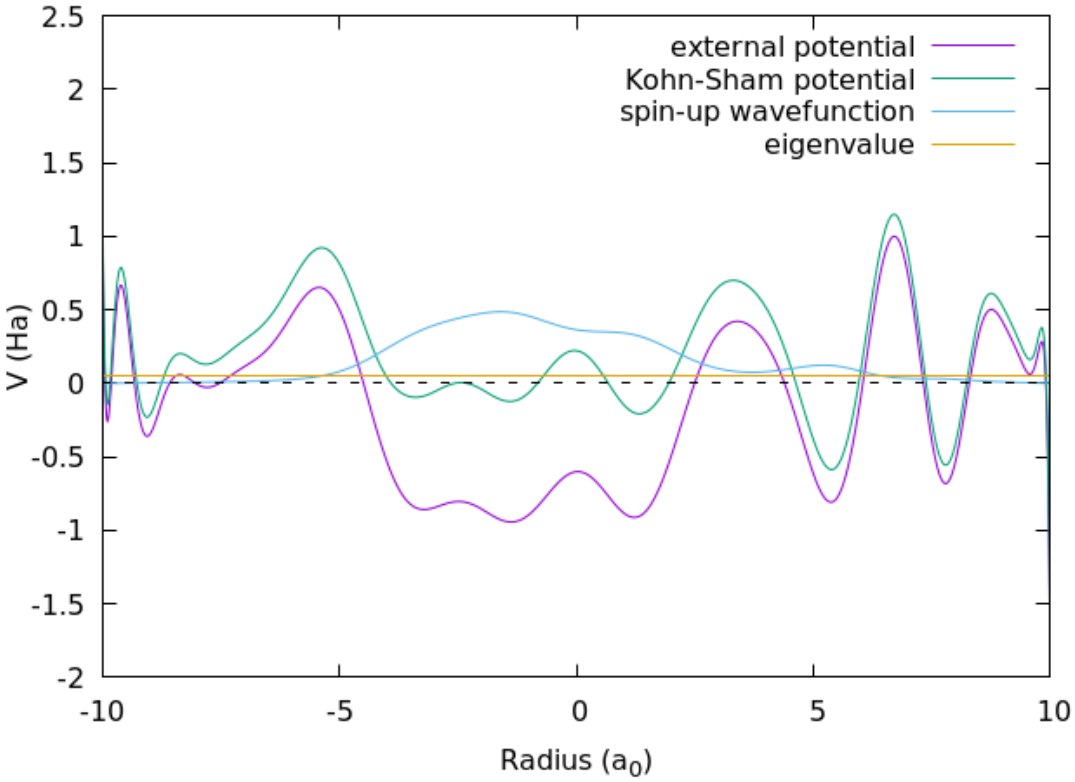

Figure B.5: Potential energy vs position on the grid for the fifth-best individual after convergence in the case of individual length 29 of a two interacting-electron system. The eigenvalue for both electrons is 0.053917 Ha. The absolute value of beta for this case was $|\beta| = 1.28 \times 10^{15}$ a.u.

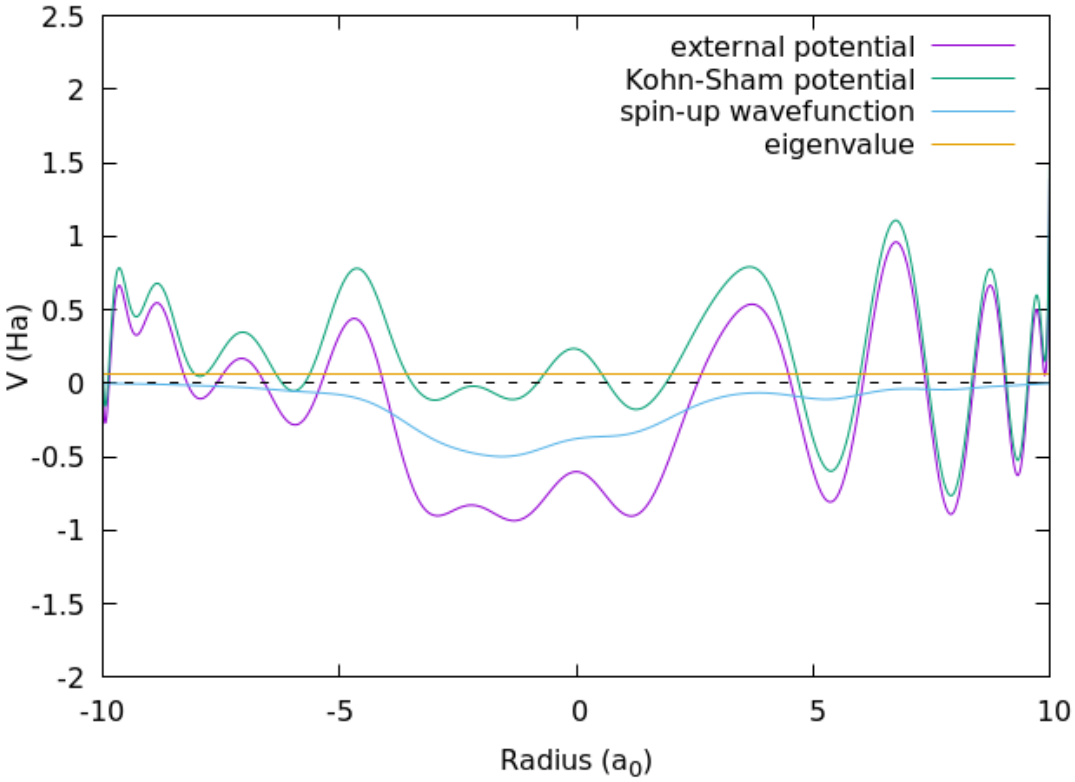

Figure B.6: Potential energy vs position on the grid for the sixth-best individual after convergence in the case of individual length 29 of a two interacting-electron system. The eigenvalue for both electrons is 0.066969 Ha. The absolute value of beta for this case was $|\beta| = 1.19 \times 10^{15}$ a.u.

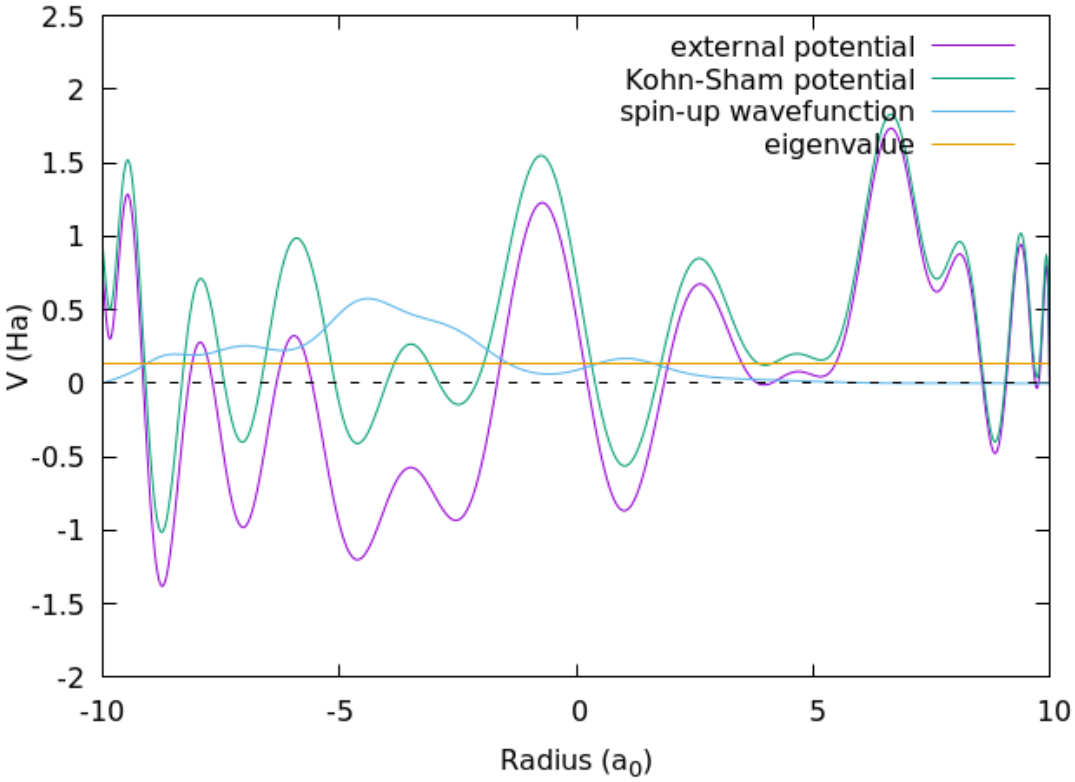

Figure B.7: Potential energy vs position on the grid for the seventh-best individual after convergence in the case of individual length 29 of a two interacting-electron system. The eigenvalue for both electrons is 0.133407 Ha. The absolute value of beta for this case was $|\beta| = 7.11 \times 10^{14}$ a.u.

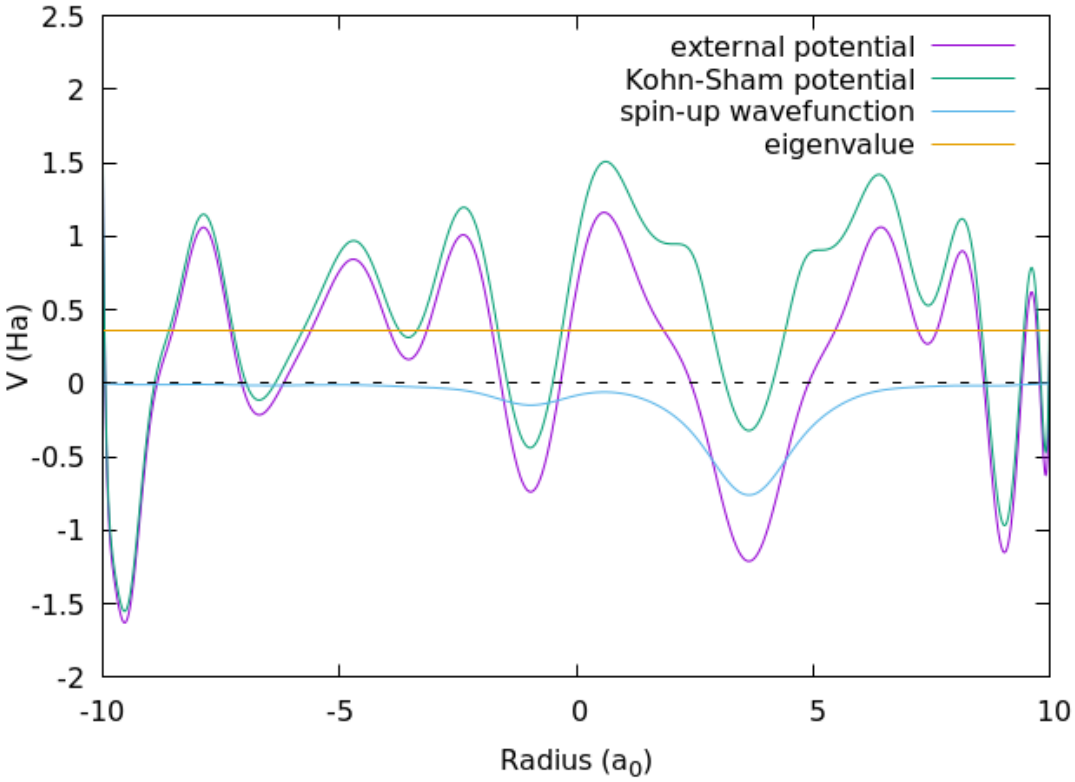

Figure B.8: Potential energy vs position on the grid for the eighth-best individual after convergence in the case of individual length 29 of a two interacting-electron system. The eigenvalue for both electrons is 0.355154 Ha. The absolute value of beta for this case was $|\beta| = 3.64 \times 10^{14}$ a.u.

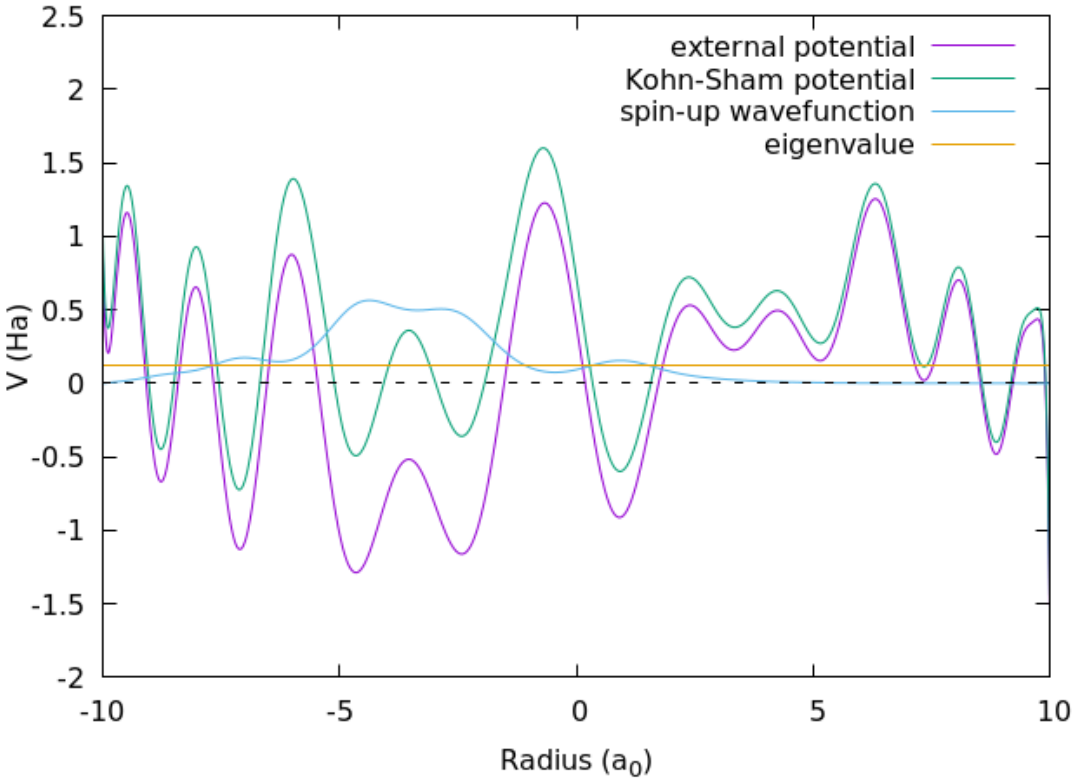

Figure B.9: Potential energy vs position on the grid for the ninth-best individual after convergence in the case of individual length 29 of a two interacting-electron system. The eigenvalue for both electrons is 0.121564 Ha. The absolute value of beta for this case was $|\beta| = 3.63 \times 10^{14}$ a.u.

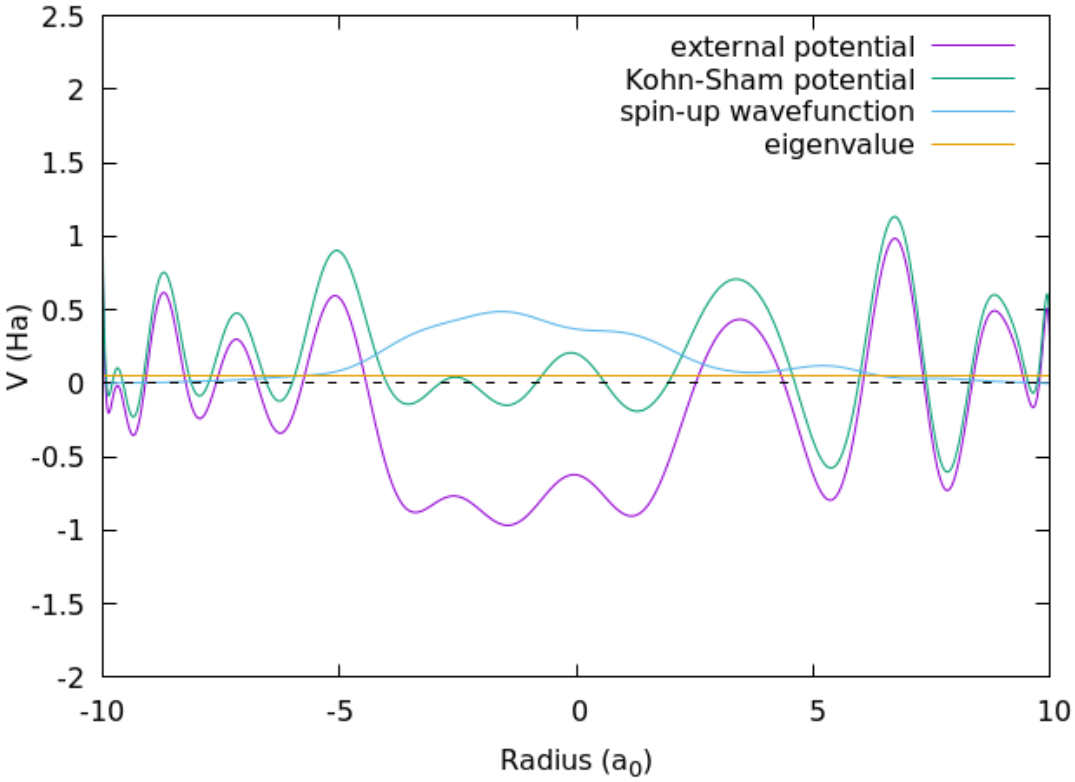

Figure B.10: Potential energy vs position on the grid for the tenth-best individual after convergence in the case of individual length 29 of a two interacting-electron system. The eigenvalue for both electrons is 0.049559 Ha. The absolute value of beta for this case was $|\beta| = 2.40 \times 10^{14}$ a.u.

Bibliography

[1] M.A.L. Marques et. al. *Fundamentals of Time-Dependent Density Functional Theory*. Springer-Verlag Berlin Heidelberg, 2012.

[2] Michele Casula, Sandro Sorella, and Gaetano Senatore. "Ground state properties of the one-dimensional Coulomb gas using the lattice regularized diffusion Monte Carlo method". In: *Phys. Rev. B* 74 (24 Dec. 2006), p. 245427. DOI: 10.1103/PhysRevB.74.245427. URL: https://link.aps.org/doi/10.1103/PhysRevB.74.245427.

[3] R.M. Dreizler and E.K.U. Gross. *Density Functional Theory: An Approach to the Quantum Many-Body Problem*. Springer Berlin Heidelberg, 2012.

[4] C. Fiolhais, F. Nogueira, and M.A.L. Marques. *A Primer in Density Functional Theory*. Springer-Verlag Berlin Heidelberg, 2003.

[5] X. Gonze and J.-P. Vigneron. "Density-functional approach to nonlinear-response coefficients of solids". In: *Phys. Rev. B* 39 (18 June 1989), pp. 13120–13128. DOI: 10.1103/PhysRevB.39.13120. URL: https://link.aps.org/doi/10.1103/PhysRevB.39.13120.

[6] P. Hohenberg and W. Kohn. "Inhomogeneous Electron Gas". In: *Phys. Rev.* 136 (3B Nov. 1964), B864–B871. DOI: 10.1103/PhysRev.136.B864. URL: https://link.aps.org/doi/10.1103/PhysRev.136.B864.

[7] Mark Kuzyk. "Physical Limits on Electronic Nonlinear Molecular Susceptibilities". In: *Physical review letters* 85 (Sept. 2000), pp. 1218–21. DOI: 10.1103/PhysRevLett.85.1218.

[8] Mark G. Kuzyk. "Fundamental limits of all nonlinear-optical phenomena that are representable by a second-order nonlinear susceptibility". In: *The Journal of Chemical Physics* 125.15 (2006), p. 154108. DOI: 10.1063/1.2358973. URL: https://doi.org/10.1063/1.2358973.

[9] Mark G. Kuzyk. "Using fundamental principles to understand and optimize nonlinear-optical materials". In: *J. Mater. Chem.* 19 (40 2009), pp. 7444–7465. DOI: 10.1039/B907364G. URL: http://dx.doi.org/10.1039/B907364G.

[10] Mark G. Kuzyk et al. "Using numerical optimization techniques and conjugation modulation to design the ultimate nonlinear-optical molecule". In: Optical Society of America, July 2007, WC1. DOI: 10.1364/NLO.2007.WC1. URL: http://www.osapublishing.org/abstract.cfm?URI=NLO-2007-WC1.

[11] M.G. Kuzyk. "Quantum limits of the hyper-Rayleigh scattering susceptibility". In: *IEEE Journal of Selected Topics in Quantum Electronics* 7.5 (2001), pp. 774–780. DOI: 10.1109/2944.979338.

[12] Robert van Leeuwen. "Mapping from Densities to Potentials in Time-Dependent Density-Functional Theory". In: *Phys. Rev. Lett.* 82 (19 May 1999), pp. 3863–3866. DOI: 10.1103/PhysRevLett.82.3863. URL: https://link.aps.org/doi/10.1103/PhysRevLett.82.3863.

[13] C Legrand, E Suraud, and P-G Reinhard. "Comparison of self-interaction-corrections for metal clusters". In: *Journal of Physics B: Atomic, Molecular and Optical Physics* 35.4 (Feb. 2002), pp. 1115–1128. DOI: 10.1088/0953-4075/35/4/333. URL: https://doi.org/10.1088/0953-4075/35/4/333.

[14] R.G. Parr and Y. Weitao. *Density-Functional Theory of Atoms and Molecules*. International Series of Monographs on Chemistry. Oxford University Press, 1994.

[15] Giancarlo Strinati. "Application of the Green's functions method to the study of the optical properties of semiconductors". In: *La Rivista del Nuovo Cimento* 11 (Dec. 1988), pp. 1–86. DOI: 10.1007/BF02725962.

[16] Attila Szabo and Neil S. Ostlund. *Modern Quantum Chemistry : Introduction to Advanced Electronic Structure Theory*. Dover Publications, Inc., 1996.

[17] Urszula Szafruga, Mark Kuzyk, and David Watkins. "Maximizing the hyperpolarizability of one-dimensional systems". In: *Journal of Nonlinear Optical Physics & Materials* 19 (Mar. 2010). DOI: 10.1142/S0218863510005303.

[18] Carsten A. Ullrich. *Time-Dependent Density-Functional Theory: Concepts and Applications*. Oxford University Press, 2012.

[19] Tiecheng Wang and Shihao Zhang. "Large enhancement of second harmonic generation from transition-metal dichalcogenide monolayer on grating near bound states in the continuum". In: *Opt. Express* 26.1 (Jan. 2018), pp. 322–337. DOI: 10.1364/OE.26.000322. URL: http://www.opticsexpress.org/abstract.cfm?URI=oe-26-1-322.

[20] David Watkins and Mark Kuzyk. "The effect of electron interactions on the universal properties of systems with optimized intrinsic off-resonant hyperpolarizability". In: *The Journal of chemical physics* 134 (Mar. 2011), p. 094109. DOI: 10.1063/1.3560031.

[21] Juefei Zhou, Mark G. Kuzyk, and David S. Watkins. "Pushing the hyperpolarizability to the limit". In: *Opt. Lett.* 31.19 (Oct. 2006), pp. 2891–2893. DOI: 10.1364/OL.31.002891. URL: http://ol.osa.org/abstract.cfm?URI=ol-31-19-2891.

[22] Juefei Zhou et al. "Optimizing potential energy functions for maximal intrinsic hyperpolarizability". In: *Physical Review A - PHYS REV A* 76 (Nov. 2007), pp. 053831–053831. DOI: 10.1103/PHYSREVA.76.053831.